AIP | Journal of Applied Physics

Beam coupling in hybrid photorefractive inorganic-cholesteric liquid crystal cells: Impact of optical rotation

V. Yu. Reshetnyak, I. P. Pinkevych, T. J. Sluckin, G. Cook, and D. R. Evans

Citation: Journal of Applied Physics **115**, 103103 (2014); doi: 10.1063/1.4867479
View online: http://dx.doi.org/10.1063/1.4867479
View Table of Contents: http://scitation.aip.org/content/aip/journal/jap/115/10?ver=pdfcov
Published by the AIP Publishing

Beam coupling in hybrid photorefractive inorganic-cholesteric liquid crystal cells: Impact of optical rotation

V. Yu. Reshetnyak,[1] I. P. Pinkevych,[1] T. J. Sluckin,[2] G. Cook,[3] and D. R. Evans[3]
[1]*Physics Faculty, National Taras Shevchenko University of Kyiv, Volodymyrs'ka Street 64, Kyiv 01601, Ukraine*
[2]*Division of Mathematical Sciences, University of Southampton, Highfield, Southampton SO17 1BJ, United Kingdom*
[3]*Air Force Research Laboratory, Materials and Manufacturing Directorate, Wright-Patterson Air Force Base, Ohio 45433, USA*

(Received 28 October 2013; accepted 20 February 2014; published online 11 March 2014)

We develop a theoretical model to describe two-beam energy exchange in a hybrid photorefractive inorganic-cholesteric cell. A cholesteric layer is placed between two inorganic substrates. One of the substrates is photorefractive (Ce:SBN). Weak and strong light beams are incident on the hybrid cell. The interfering light beams induce a periodic space-charge field in the photorefractive window. This penetrates into the cholesteric liquid crystal (LC), inducing a diffraction grating written on the LC director. In the theory, the flexoelectric mechanism for electric field-director coupling is more important than the LC static dielectric anisotropy coupling. The LC optics is described in the Bragg regime. Each beam induces two circular polarized waves propagating in the cholesteric cell with different velocities. The model thus includes optical rotation in the cholesteric LC. The incident light beam wavelength can fall above, below, or inside the cholesteric gap. The theory calculates the energy gain of the weak beam, as a result of its interaction with the pump beam within the diffraction grating. Theoretical results for exponential gain coefficients are compared with experimental results for hybrid cells filled with cholesteric mixture BL038/CB15 at different concentrations of chiral agent CB15. Reconciliation between theory and experiment requires the inclusion of a phenomenological multiplier in the magnitude of the director grating. This multiplier is cubic in the space-charge field, and we provide a justification of the q-dependence of the multiplier. Within this paradigm, we are able to fit theory to experimental data for cholesteric mixtures with different spectral position of cholesteric gap relative to the wavelength of incident beams, subject to the use of some fitting parameters. © *2014 AIP Publishing LLC*. [http://dx.doi.org/10.1063/1.4867479]

I. INTRODUCTION

Significant progress has been made in recent years in the study of liquid crystal (LC) photorefractive cells. These cells are used in beam-coupling experiments, and it is of interest to understand particular liquid crystal properties which optimize the beam-coupling effect. This involves not only adding molecular chiral dopants (or switching to a chiral nematic compound) but also the addition of various types of impurity, including nanocolloids of various types.

In this paper, we study hybrid organic-inorganic photorefractives, in which a LC sample is placed adjacent to a photorefractive layer containing photo-generated space charges. A whole set of analogous photorefractive liquid crystalline systems have been treated in the literature.[1–6] The resulting space-charge electric fields then penetrate into the adjacent LC, causing a director-modulation-induced grating. The incident light beams are diffracted by the grating, leading to an exchange of intensity between them. One of the beams is amplified, and in a LC beam-coupling geometry the exponential gain coefficients can reach values more than two orders of magnitude larger than those in solid inorganic photorefractive crystals.[7–12] Many of these systems involve a thin LC sample between two photorefractive layers. This is the so-called "dual photorefractive window geometry," and can be contrasted with the "single photorefractive window geometry," in which a photorefractive slab is present on only one side of the liquid crystal cell.

Theoretical models for these systems were first developed by Tabiryan and Umeton,[13] and by Jones and Cook,[14] who supposed the beam-coupling mechanisms in hybrid organic-inorganic photorefractives to be similar to those in conventional LC cells. Coupling between the director and the light-induced space-charge electric field would then be caused by the LC static dielectric anisotropy. This hypothesis predicts the maximal energy transfer to occur when the grating spacing and the LC cell thickness are of comparable dimension. But apparently this is not the case.[10–12] Rather, this maximum occurs when the ratio of grating spacing to cell thickness is rather small.

The present authors have carried out some previous studies of these systems.[15–17] The maximal energy transfer paradox has been resolved, but involves two unexpected phenomena. One is that the director deformation is governed by the flexoelectric interactions, rather than by static dielectric anisotropy coupling. The second is that the magnitude of the director grating is a non-linear function of the space-charge electric field. In Ref. 15, we have discussed possible mechanisms for this puzzling nonlinearity.

In Ref. 16, we have extended previous experimental beam-coupling studies to hybrid cholesteric LC cells. These systems exhibit a significant additional feature not observed in hybrid nematic LC cells. Here, the sign of the gain coefficient changes as the grating spacing is increased. In Ref. 17, we have extended Ref. 15 in order to address this problem. Theory and experiment are in qualitative agreement, if optical rotation can be neglected, and if nematic regions very close to the surfaces shield the surfaces from the bulk chiral system. This might be the consequence of chiral molecule segregation following from director-concentration coupling.

Here, we discuss a particular set of experimental results[16] obtained in a single photorefractive window geometry. In these experiments, the wavelength of the incident linearly polarized wave falls either in the cholesteric gap or very close to it, and is close to the pitch of the cholesteric sample. However, the theory developed in Ref. 17, although in principle applicable, fails to describe these results. In Fig. 1, we compare the results of the experiments with predictions generated by the theory of Ref. 17, for two values of the cholesteric pitch.

This resolution of the apparent paradox principally involves a more accurate description of the chiral nature of the material. The single window geometry permits observations in which optical rotation is significant. In the cholesteric gap regime, we may recall, the cholesteric reflects almost completely one circular polarization optical mode, while transmitting the other. The correct model of beam-coupling involves, in addition to elements discussed previously, the decomposition of the incident linear polarized beam into its two circularly polarized components, and an explicit treatment of polarization rotation inside the sample. In addition, to fit the experimental data, we also have to modify slightly the details of the non-linear dependence of the magnitude of the director grating on the space-charge electric field discussed in Ref. 15. Our analysis not only explains the experiments for wavelengths in the cholesteric gap but also provides an alternative explanation of data previously discussed.[17]

The paper is organized as follows. In Sec. II, we introduce the model of hybrid cholesteric cell in the field of the interfering incident light beams and define the evanescent photorefractive field in the LC cell. In Sec. III, we derive equations for the LC director subject to this electric field and solve them. In Sec. IV, we discuss light propagation in the LC, starting with expressions for the dielectric tensor, going on to equations for the two coupled light modes and expressions for the exponential gain coefficient in the LC cell. In Sec. V, we make comparisons with experimental results and in Sec. VI present some brief conclusions.

II. PHOTOREFRACTIVE ELECTRIC FIELD IN LIQUID CRYSTAL CELL

Let the z-axis be directed perpendicular to the planes of hybrid photorefractive cell and the cholesteric LC is bounded by the planes $z = -L/2$ and $z = L/2$ (Fig. 2). The director boundary conditions are homogeneous in the x-direction (in-plane). We shall suppose that the cholesteric pitch inside the cell is uniform. This requires that there are an integer number n of chiral director twists between the cell walls. If the cholesteric pitch is p, then $2p = nL$. We remark that, in practice, the thickness of the cell will not be exactly commensurate with the equilibrium cholesteric pitch, and that in order to fit an integral number of rotations into the sample, the value of the pitch in the sample will be slightly displaced from its equilibrium value. This problem has been addressed in the literature[18–20] but we shall not address it here, as it is not directly pertinent to the present optical study. A further complicating factor is possible non-uniformity of the helical pitch, induced by non-uniformity in the chiral dopant concentration, which we shall similarly neglect. We note, however, that in practice, this is also likely to be present, and indeed we have invoked this possibility in our previous study[17] of two-beam coupling in cholesteric mixtures away from the cholesteric gap.

The hybrid cell is illuminated by two intersecting coherent light beams $\mathbf{E}_1 = A_1\mathbf{e}_1\exp(i\mathbf{k}_1\boldsymbol{r} - i\omega t)$ and $\mathbf{E}_2 = A_2\mathbf{e}_2\exp(i\mathbf{k}_2\boldsymbol{r} - i\omega t)$. The bisector of the beams is directed along the z-axis, and the wave vectors $\mathbf{k}_1, \mathbf{k}_2$ lie in the xz-plane. On the entrance plane $z = -L/2$, the polarization vectors $\mathbf{e}_1, \mathbf{e}_2$ of the beams lie in the xz-plane. As the

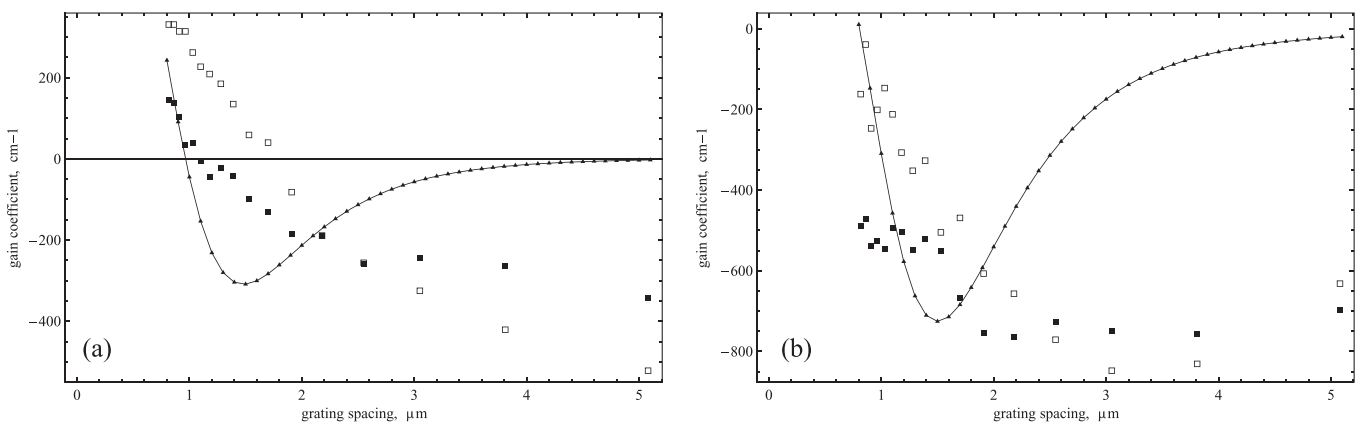

FIG. 1. Gain coefficient versus grating spacing: comparison of theory[17] with experiments[16] for 5 μm hybrid cell filled with cholesteric mixture BL038/CB15, showing inadequacy of previous theory. Note particularly that trends are incorrectly predicted. (a) cholesteric pitch: p = 0.44 μm, (b), p = 0.65 μm. Legend: theory from Ref. 17—curves; experimental data[16]—boxes.

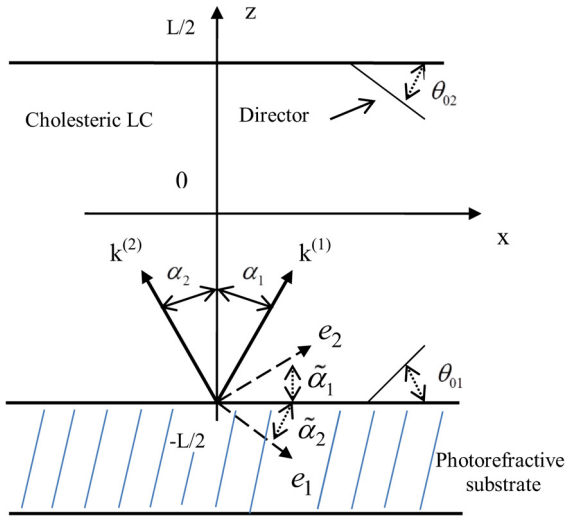

FIG. 2. Cholesteric LC cell, showing light beams incident from photorefractive medium, together with associated wave- and polarization vectors. The quantities $\mathbf{k}^{(1,2)}$,$\alpha_{1,2}$,$\tilde{\alpha}_{1,2}$,$\mathbf{e}_{1,2}$,$\theta_{01,2}$ are defined in the text. By convention, we suppose beam 1 to be the signal beam, and beam 2 to be the pump.

beams propagate across the cholesteric cell, however, they can rotate. On the exit plane $z = L/2$, the polarization plane may, in general, possess an orientation different from that on the entrance plane.

For cells with two photorefractive substrates, the entrance and exit photorefractive substrates are then illuminated by light fields with different polarizations. The photorefractive electric field arising in the photorefractive substrates thus possess unequal orientations, which complicates the analysis of the diffraction grating.[15,17] However, in the experimental setup considered here, the hybrid photorefractive cell contains only a single photorefractive substrate (Ce:SBN) deposited on the entrance plane at $z = -L/2$. The exit substrate siding at $z = L/2$ is non-photorefractive (glass).

The beams produce a light intensity interference pattern in the photorefractive substrate for $z \le -L/2$,

$$I(z) = (I_1 + I_2)\left[1 + \frac{1}{2}(m\exp(iqx) + c.c.)\right], \qquad (1)$$

where we define the modulation parameter $m = 2\cos(2\delta)A_1A_2^*/(I_1 + I_2)$, and where 2δ is the angle between incident beams in the photorefractive medium, $I_1 = A_1A_1^*$, $I_2 = A_2A_2^*$ are the intensities of incident beams, and $q = k_{1x} - k_{2x} = 2k\sin\delta \approx 2k\delta$ is the wave number of the intensity pattern. We shall focus particularly on the interference pattern on the photorefractive medium-LC boundary (i.e., as the light beams enter the liquid); here, we denote

$$m \equiv m(-L/2) = 2\cos(2\delta)A_1(-L/2)A_2^*(-L/2)/(I_1 + I_2). \qquad (2)$$

The quantity $m = m(-L/2)$ plays a particularly important role in the theory and will recur frequently in the ensuing analysis.

Inside the photorefractive substrate, the light intensity pattern given by Eq. (1) induces a space charge. The space-charge density is modulated along the x-axis with period equal to $2\pi/q$ and gives rise to an electric potential $\tilde{\Phi}(x)$ at the cell boundary:

$$\tilde{\Phi}(x) = \tilde{\Phi}_0 + \left[\tilde{\Phi}\exp(iqx) + c.c.\right], \qquad (3)$$

where $\tilde{\Phi}_0$ is an arbitrary constant (which may be taken to be zero), and

$$\tilde{\Phi} = \frac{iE_{sc}(q)}{2q}m. \qquad (4)$$

In particular, in an infinite photorefractive medium and for a diffusion-dominated space-charge field $E_{sc}(q)$ takes the following form:[21]

$$E_{sc}(q) = \frac{iE_d}{1 + \frac{E_d}{E_q}}, \quad E_d = q\frac{k_bT}{e}, \quad E_q = \left(1 - \frac{N_a}{N_d}\right)\frac{eN_a}{\varepsilon_0\varepsilon_{Ph}q}, \qquad (5)$$

where E_d is the diffusion field, E_q is the so-called saturation field, N_a and N_d are, respectively, the acceptor and donor impurity densities, ε_{Ph} is the dielectric permittivity of photorefractive material, and e is the electron charge.

The space-charge electric field penetrates from photorefractive substrate into the flexoelectric cholesteric LC. The photorefractive medium is not infinite, but rather semi-infinite. The solution for the electric fields in the photorefractive substrate and the LC is actually a complex coupled problem. However, if we suppose that Eqs. (3)–(5) remain valid at the liquid-crystal-photorefractive medium boundary, the electric field problems in the two media separate, with Eqs. (3)–(5) now acting as boundary conditions for the electric potential within the LC cell.

Finally, we note director pretilt at the LC cell boundaries, which we describe, respectively, by angles θ_{01}, θ_{02} in the xz-plane.

The electric field in the cholesteric LC cell can be found from the Poisson equation

$$\nabla \cdot (\varepsilon_0\hat{\tilde{\varepsilon}} \cdot \mathbf{E} + \mathbf{P}_f) = 0, \qquad (6)$$

where the flexopolarization $\mathbf{P}_f$ is defined by the expression $\mathbf{P}_f = e_1\mathbf{n}\nabla\cdot\mathbf{n} + e_3(\nabla\times\mathbf{n}\times\mathbf{n})$,[22] $\tilde{\varepsilon}_{ij} = \tilde{\varepsilon}_\perp\delta_{ij} + \tilde{\varepsilon}_a n_i n_j$ is the low frequency dielectric permittivity of the cholesteric LC, n_i are the components of the director $\mathbf{n}$, $\tilde{\varepsilon}_a = \tilde{\varepsilon}_\parallel - \tilde{\varepsilon}_\perp$ is the dielectric anisotropy, $\tilde{\varepsilon}_\parallel$ and $\tilde{\varepsilon}_\perp$ are the components of the dielectric tensor along and perpendicular to the director, e_1 and e_3 are the flexoelectric coefficients.

To solve Eq. (6) inside the cholesteric LC, we use the relation $\mathbf{E}(x,z) = -\nabla\Phi(x,z)$, and seek solutions for the electric potential $\Phi(x,z)$ in the form

$$\Phi(x,z) = \Phi_0(z) + \left[\Phi(z)\exp(iqx) + c.c.\right]. \qquad (7)$$

We note that the director field $\mathbf{n}(\boldsymbol{r})$ responds to the electric field defined in Eq. (6), and that, generally speaking, it is necessary to solve Eq. (6) self-consistently with equations for the director. However, we will consider only small

deviations of the director in response to the electric field. In this case, we can neglect the feedback of the director response on the electric field and influence of small angles of the director pretilt at the cell boundaries.

Combining Eqs. (6) and (7), we derive

$$\frac{\partial^2}{\partial z^2}\Phi_0(z) = 0, \tag{8}$$

$$\frac{\partial^2}{\partial z^2}\Phi(z) + \left[-\frac{\tilde{\varepsilon}_{\parallel}+\tilde{\varepsilon}_{\perp}}{2\tilde{\varepsilon}_{\perp}}q^2 - \frac{\tilde{\varepsilon}_a q^2}{2\tilde{\varepsilon}_{\perp}}\cos 2\varphi_0(z)\right]\Phi(z) = 0, \tag{9}$$

where

$$\varphi_0(z) = \frac{2\pi}{p}(z + L/2), \tag{10}$$

and p is the pitch of the cholesteric helix.

Using Eqs. (3)–(5), the boundary conditions for the electric potentials at the LC boundaries $z = \mp\frac{L}{2}$ can now be written as

$$\Phi_0(z = \mp L/2) = 0, \quad \Phi(z = -L/2) = \frac{iE_{sc}(q)}{2q}m,$$
$$\Phi(z = L/2) = 0. \tag{11}$$

Equation (9) is Mathieu's equation.[23] For parameters used in our theory, the second term in square brackets is small in comparison with the first term over most of the range of angle φ_0. Then, to simplify further calculation, we replace this second term by its average value which equals zero, yielding

$$\frac{\partial^2}{\partial z^2}\Phi(z) - \frac{\tilde{\varepsilon}_{\parallel}+\tilde{\varepsilon}_{\perp}}{2\tilde{\varepsilon}_{\perp}}q^2\Phi(z) = 0. \tag{12}$$

We solve Eqs. (8) and (12) with boundary conditions (11), yielding the following expressions for electric field in the LC cell:

$$\begin{aligned} E_x &= E_{0x}\exp(iqx) + c.c, \\ E_z &= E_{0z}\exp(iqx) + c.c., \end{aligned} \tag{13}$$

$$E_{0x} = -\frac{E_{sc}(q)m}{2\sinh(\tilde{q}L)}\sinh\tilde{q}(z - L/2),$$
$$E_{0z} = \frac{i\tilde{q}E_{sc}(q)m}{2q\sinh(\tilde{q}L)}\cosh\tilde{q}(z + L/2), \tag{14}$$

where $\tilde{q} = q\sqrt{\frac{\tilde{\varepsilon}_{\perp}+\tilde{\varepsilon}_{\parallel}}{2\tilde{\varepsilon}_{\perp}}}$.

III. CHOLESTERIC LC DIRECTOR PROFILE

The equilibrium director profile can be found by minimizing the total free energy functional of the cholesteric LC cell defined by

$$F = F_{el} + F_l + F_E + F_{fl}, \tag{15}$$

where

$$F_{el} = \frac{1}{2}\int\left[K_{11}(\nabla\cdot\mathbf{n})^2 + K_{22}(\mathbf{n}\cdot\nabla\times\mathbf{n} + g)^2 + K_{33}(\mathbf{n}\times\nabla\times\mathbf{n})^2\right]dV, F_l = -\frac{\varepsilon_0\varepsilon_a}{4}\int(\mathbf{n}\cdot\mathbf{E}_{h\nu})^2 dV,$$
$$F_E = -\frac{1}{2}\int(\mathbf{D}\cdot\mathbf{E})^2 dV, F_{fl} = -\int(\mathbf{P}_f\cdot\mathbf{E})\,dV. \tag{16}$$

The meaning of the quantities in Eq. (16) is as follows:

a) F_{el} is the bulk elastic energy of a distorted cholesteric LC layer;
b) F_l is contribution of the light field to the total free energy functional;
c) F_E is the contribution from the dc-electric field created in the LC cell by the photorefractive layers;
d) F_{fl} is the contribution from interaction of the dc-electric field with the LC flexoelectric polarization;
e) K_{11}, K_{22}, K_{33} are the splay, twist, and bend elastic constants, respectively;
f) $g = \frac{2\pi}{p}$, with p the cholesteric pitch;
g) ε_a is the anisotropy of the LC dielectric permittivity at optical frequency;
h) $\mathbf{E}_{h\nu}$ is the electric vector of the light field in the cholesteric LC.

Finally, we suppose infinitely rigid director anchoring on the cell surfaces $z = \mp L/2$ with director pretilt angles in the xz-plane θ_{01}, θ_{02}, respectively (Fig. 2).

Some terms in Eqs. (15) and (16) can now be neglected. The optical frequency LC dielectric anisotropy $\varepsilon_a \ll 1$, implying neglect of the light field contribution F_l. The LC dielectric anisotropy term F_E can be neglected with respect to the LC flexopolarization. We refer readers to Refs. 15 and 17 for a more detailed justification. For simplicity, we suppose $K_{11} = K_{22} = K_{33} = K$ (see also Sala and Karpierz[24] for a more detailed discussion of the status of the one-constant approximation in an optical context).

It is convenient to parameterize the director in the form $\mathbf{n} = (\cos\varphi(x,z)\sin\beta(x,z),\ \sin\varphi(x,z)\sin\beta(x,z),\ \cos\beta(x,z))$, where $\beta(x,z)$ is the director polar angle with the z-axis and $\varphi(x,z)$ is the director azimuth angle with respect to the x-axis. We can then define $\vartheta(x,z)$ by $\vartheta(x,z) = \frac{\pi}{2} - \beta(x,z)$, where $\vartheta(x,z)$ is a small reorientation with respect to the xy-plane, with $\vartheta(x,z) = \theta_0(z) + [\theta(z)\exp(iqx) + c.c.]$. Likewise, we can decompose the azimuthal director angle $\varphi(x,z) = \varphi_0(z) + [\varphi(z)\exp(iqx) + c.c.]$ into a mean value and superimposed fluctuations.

After some straightforward algebra, the linearized Euler-Lagrange equations for $\theta(z)$, $\varphi(z)$,and $\theta_0(z)$ appropriate to the free energy functional Eq. (15) are now

$$\frac{\partial^2\theta}{\partial z^2} - \left(q^2+g^2\right)\theta = r\left[iq\cos\varphi_0 \mathrm{E}_{0z} + \left(\frac{\partial \mathrm{E}_{0z}}{\partial z} - iq\cos^2\varphi \mathrm{E}_{0x}\right)\theta_0\right] - r_1 g\sin\varphi_0 \mathrm{E}_{0x}, \tag{17}$$

$$\frac{\partial^2\varphi}{\partial z^2} - q^2\varphi = -iqr\left(\frac{1}{2}\sin 2\varphi_0 E_{0x} + \theta_0\sin\varphi_0 E_{0z}\right) + r_1\sin\varphi_0\frac{\partial\theta_0}{\partial z}E_{0x}, \tag{18}$$

$$\frac{\partial^2\theta_0}{\partial z^2} - g^2\theta_0 = 0, \tag{19}$$

where $r = \frac{e_1+e_3}{K}$, $r_1 = \frac{e_1-e_3}{K}$. The boundary conditions for Eqs. (17)–(19) are

$$\theta(\mp L/2) = 0, \quad \varphi(\mp L/2) = 0, \quad \theta_0(-L/2) = \theta_{01}, \quad \theta_0(L/2) = \theta_{02}. \tag{20}$$

In our solutions to Eq. (17), we neglect terms of $o(\theta_0^2)$. Equation (30) below for the dielectric constant requires only terms of $o(\theta_0)$. In addition, we note that in the experiments[16] the condition $qL \gg 1$, $gL \gg 1$ is satisfied. Considering only this case, we can simplify expressions for solutions to Eqs. (17) and (18) by neglecting terms of higher order in e^{-qL}, e^{-gL}. The solution to Eq. (17), subject to these restrictions, is given by

$$\theta(z) = \frac{iE_{sc}(q)}{2q}d(z)m, \tag{21}$$

where

$$d(z) = [e^{-(\tilde{q}-ig)z} - e^{-(\tilde{q}-ig+\sqrt{q^2+g^2})L/2}e^{\sqrt{q^2+g^2}z} - e^{(\tilde{q}-ig-\sqrt{q^2+g^2})L/2}e^{-\sqrt{q^2+g^2}z}]\frac{(r_1 g + ir\tilde{q})qe^{(ig-\tilde{q})L/2}}{2[\tilde{q}^2 - q^2 - 2g^2 - 2i\tilde{q}g]} - c.c., \tag{22}$$

$$\varphi(z) = \frac{iE_{sc}(q)}{2q}f(z)m, \tag{23}$$

where

$$f(z) = \frac{1}{4}\frac{i(-1)^n rq\tilde{q}e^{-\tilde{q}L/2}}{(\tilde{q}^2 - q^2 - 4g^2)^2 + 16g^2\tilde{q}^2}[(\tilde{q}^2 - q^2 - 4g^2 + i4g\tilde{q})e^{(-\tilde{q}+i2g)z} - (\tilde{q}^2 - q^2 - 4g^2 - i4g\tilde{q})e^{(-\tilde{q}-i2g)z} - i8g\tilde{q}(-1)^n(e^{-\tilde{q}L/2}e^{q(z-L/2)} + e^{\tilde{q}L/2}e^{-q(z+L/2)})] - \frac{q}{2}e^{-(\tilde{q}+g)L/2}[\theta_{01}F(z,g) - \theta_{02}F(z,-g)], \tag{24}$$

$$F(z,g) = \frac{(r\tilde{q} - r_1 g)[(\tilde{q}^2 - q^2 + 2\tilde{q}g) + 2ig(\tilde{q}+g)]e^{(\tilde{q}+g)L/2}}{(\tilde{q}^2 - q^2 + 2\tilde{q}g)^2 + 4g^2(\tilde{q}+g)^2}[e^{-(\tilde{q}+g-ig)(z+L/2)} - (-1)^n e^{-(\tilde{q}+g)L}e^{q(z-L/2)} - e^{-q(z+L/2)}] - c.c. \tag{25}$$

$$\theta_0(z) = \theta_{01}e^{-g(z+L/2)} + \theta_{02}e^{g(z-L/2)}. \tag{26}$$

IV. COUPLED LIGHT MODES

A. General expression for cholesteric dielectric tensor

Using the definition of the cholesteric LC director by the director angles $\theta(x,z)$ and $\varphi(x,z)$, $\mathbf{n} = (\cos\varphi(x,z)\cos\theta(x,z), \sin\varphi(x,z)\cos\theta(x,z), \sin\theta(x,z))$, the optical frequency dielectric tensor $\varepsilon_{ij} = \varepsilon_\perp\delta_{ij} + \varepsilon_a n_i n_j$, takes the form

$$\hat{\varepsilon} = \begin{vmatrix} \varepsilon_\perp + \varepsilon_a\cos^2\varphi(x,z)\cos^2\theta(x,z) & \frac{1}{2}\varepsilon_a\sin 2\varphi(x,z)\cos^2\theta(x,z) & \frac{1}{2}\varepsilon_a\cos\varphi(x,z)\sin 2\theta(x,z) \\ \frac{1}{2}\varepsilon_a\sin 2\varphi(x,z)\cos^2\theta(x,z) & \varepsilon_\perp + \varepsilon_a\sin^2\varphi(x,z)\cos^2\theta(x,z) & \frac{1}{2}\varepsilon_a\sin\varphi(x,z)\sin 2\theta(x,z) \\ \frac{1}{2}\varepsilon_a\cos\varphi(x,z)\sin 2\theta(x,z) & \frac{1}{2}\varepsilon_a\sin\varphi(x,z)\sin 2\theta(x,z) & \varepsilon_\perp + \varepsilon_a\sin^2\theta(x,z) \end{vmatrix}. \tag{27}$$

Substituting $\vartheta(x,z) = \theta_0(z) + [\theta(z)\exp(iqx) + c.c.]$, $\varphi(x,z) = \varphi_0(z) + [\varphi(z)\exp(iqx) + c.c.]$ into Eq. (27) and neglecting terms of second order and higher in the angles $\theta(z)$ and $\varphi(z)$, one can rewrite the dielectric tensor $\hat{\varepsilon}$ in Eq. (27) in the following way:

$$\hat{\varepsilon}(\mathrm{x},\mathrm{z}) = \hat{\varepsilon}_1(z) + \hat{\varepsilon}_2(z) + \left[\hat{\varepsilon}_3(z)\exp(iqx) + c.c.\right], \tag{28}$$

where

$$\hat{\varepsilon}_1 = \begin{vmatrix} \varepsilon_\perp + \varepsilon_a\cos^2\varphi_0 & \frac{1}{2}\varepsilon_a\sin 2\varphi_0 & 0 \\ \frac{1}{2}\varepsilon_a\sin 2\varphi_0 & \varepsilon_\perp + \varepsilon_a\sin^2\varphi_0 & 0 \\ 0 & 0 & \varepsilon_\perp \end{vmatrix}, \hat{\varepsilon}_2 = \varepsilon_a\theta_0(z) \begin{vmatrix} -\theta_0\cos^2\varphi_0 & -\frac{1}{2}\theta_0\sin 2\varphi_0 & \cos\varphi_0 \\ -\frac{1}{2}\theta_0\sin 2\varphi_0 & -\theta_0\sin^2\varphi_0 & \sin\varphi_0 \\ \cos\varphi_0 & \sin\varphi_0 & \theta_0 \end{vmatrix}, \tag{29}$$

$$\hat{\varepsilon}_3 = \varepsilon_a\theta(z) \begin{vmatrix} -2\theta_0\cos^2\varphi_0 & -\theta_0\sin 2\varphi_0 & \cos\varphi_0 \\ -\theta_0\sin 2\varphi_0 & -2\theta_0\sin^2\varphi_0 & \sin\varphi_0 \\ \cos\varphi_0 & \sin\varphi_0 & 2\theta_0 \end{vmatrix} + \varepsilon_a\varphi(z) \begin{vmatrix} -\sin 2\varphi_0 & \cos 2\varphi_0 & -\theta_0\sin\varphi_0 \\ \cos 2\varphi_0 & \sin 2\varphi_0 & \theta_0\cos\varphi_0 \\ -\theta_0\sin\varphi_0 & \theta_0\cos\varphi_0 & 0 \end{vmatrix}, \tag{30}$$

where $\varepsilon_a = \varepsilon_\parallel - \varepsilon_\perp$, and $\varepsilon_\parallel$,$\varepsilon_\perp$ are the principal values of the optical frequency dielectric tensor.

The first term in Eq. (28) corresponds to a LC with constant cholesteric pitch p and zero director pretilt on the cell boundaries. The second term takes into account director inhomogeneity inside the cell resulting from the nonzero director pretilt on the cell boundaries. The third term describes the dielectric tensor modulation. This is a consequence of the director modulation driven by the spatially periodic dc photorefractive electric field.

The electric field in the light beams satisfies the usual vector wave equation

$$\nabla \times \nabla \times \mathbf{E}_{h\nu} - \frac{\omega^2}{c^2}\hat{\varepsilon}(x,z)\mathbf{E}_{h\nu} = 0, \tag{31}$$

where in our case the dielectric permittivity is described by expressions (28)–(30).

B. Light beams in waveguide regime

1. Normal incidence

We will study propagation of plane polarized light beam incident normally on a cholesteric LC cell. Incident light beam is polarized along the x-axis at the cell entrance boundary $z = -L/2$.

First, we suppose that we are in waveguide regime when the eigenmodes are nearly circular. In this regime, the condition $\lambda > p\,(n_e - n_0)$ holds, where λ is the free space wavelength, and n_0, n_e are, respectively, the ordinary and extraordinary wave refraction indices. We will also neglect effects of the wave reflection from the far side of the cholesteric cell. Then in this case at the normal incidence, we have in the cholesteric medium with dielectric tensor given by $\hat{\varepsilon}_1$ (Eq. (29)) two circularly polarized modes propagating along the z-axis with magnitudes given by (see, e.g., Ref. 22; p. 277)

$$\begin{aligned} E^+ &= E_x + iE_y = A_0 e^{i(\omega/c)n^{(2)}(z+L/2)}, \\ E^- &= E_x - iE_y = A_0 e^{i(\omega/c)n^{(1)}(z+L/2)}, \end{aligned} \tag{32}$$

where $n^{(1)}$ and $n^{(2)}$ are refraction indices for circular polarized waves.

These circular polarized waves create electric fields in the cholesteric LC, with the following Cartesian components

$$E_x = \frac{E^+ + E^-}{2},\ E_y = \frac{E^+ - E^-}{2i}. \tag{33}$$

2. Oblique incidence

Now, we suppose that a light beam, polarized in the xz-plane, is incident on the cholesteric cell at a small angle α with respect to the cell normal (the z-axis). The cholesteric dielectric tensor is now given by $\hat{\varepsilon}_1 + \hat{\varepsilon}_2$ (see Eqs. (28)–(30)), where $\hat{\varepsilon}_2$ is in some sense small and of order $\varepsilon_a\theta_0$.

We now solve the relevant wave equation Eq. (31) with appropriate values of $\hat{\varepsilon}(x,z)$. The contribution from $\hat{\varepsilon}_2(z)$ is small. Neglecting reflection of the wave from the far side of the cholesteric cell, we may thus start use Eq. (33) as a zeroth order approximation in a perturbation scheme. Now, neglecting second order terms in θ_0 and α, we obtain the following expressions for the Cartesian components of the electric field:

$$\begin{aligned} E_x &= \frac{1}{2}A_0\left(e^{i(\omega/c)n^{(1)}(z+L/2)} + e^{i(\omega/c)n^{(2)}(z+L/2)}\right)e^{ik_x x}, \\ E_y &= \frac{i}{2}A_0\left(e^{i(\omega/c)n^{(1)}(z+L/2)} - e^{i(\omega/c)n^{(2)}(z+L/2)}\right)e^{ik_x x}, \\ E_z &= i\alpha\frac{n_1+n_2}{2}\frac{c}{\varepsilon_\perp\omega}\frac{\partial E_x}{\partial z} - \theta_0(z)\frac{\varepsilon_a}{\varepsilon_\perp}\left(\cos\varphi_0 E_x + \sin\varphi_0 E_y\right). \end{aligned} \tag{34}$$

We postpone the details of the calculation to Appendix A (see also discussions of oblique incidence, e.g., in Refs. 22 and 25). We remark that the x and y components of the field are given by Eqs. (32) and (33), although now modulated by an $\exp(ik_x x)$ factor.

In the case under consideration, there are two such light beams incident on this cholesteric cell boundary, with amplitudes A_1 and A_2, and angles of incidence α_1, α_2 (Fig. 2). Each beam produces a pair of circular polarized waves in the cholesteric cell. The Cartesian components of each beam are

likewise described by Eqs. (34), with refraction indices $n_i^{(1,2)}$ corresponding to each beam.

From Eq. (34), we can write the electric field vector in the cholesteric LC in the form

$$\mathbf{E}_{h\nu} = \mathbf{E}_1 + \mathbf{E}_2, \quad \mathbf{E}_1 = \mathbf{i}E_{1x} + \mathbf{j}E_{1y} + \mathbf{k}E_{1z},$$
$$\mathbf{E}_2 = \mathbf{i}E_{2x} + \mathbf{j}E_{2y} + \mathbf{k}E_{2z}, \tag{35}$$

where $\mathbf{E}_1$ and $\mathbf{E}_2$ are the electric vectors of the two light beams. Combining Eqs. (34) and (35), we obtain the Cartesian components of the light beam fields

$$E_{1x} = \frac{1}{2}A_1(e^{i(\omega/c)n_1^{(1)}(z+L/2)} + e^{i(\omega/c)n_1^{(2)}(z+L/2)})e^{ik_{1x}x},$$
$$E_{1y} = \frac{i}{2}A_1(e^{i(\omega/c)n_1^{(1)}(z+L/2)} - e^{i(\omega/c)n_1^{(2)}(z+L/2)})e^{ik_{1x}x},$$
$$E_{1z} = i\alpha_1\frac{n_1^{(1)}+n_1^{(2)}}{2}\frac{c}{\varepsilon_\perp\omega}\frac{\partial E_{1x}}{\partial z} - \theta_0(z)\frac{\varepsilon_a}{\varepsilon_\perp}(\cos\varphi_0 E_{1x} + \sin\varphi_0 E_{1y}) \tag{36}$$

and

$$E_{2x} = \frac{1}{2}A_2(e^{i(\omega/c)n_2^{(1)}(z+L/2)} + e^{i(\omega/c)n_2^{(2)}(z+L/2)})e^{ik_{2x}x},$$
$$E_{2y} = \frac{i}{2}A_2(e^{i(\omega/c)n_2^{(1)}(z+L/2)} - e^{i(\omega/c)n_2^{(2)}(z+L/2)})e^{ik_{2x}x},$$
$$E_{2z} = -i\alpha_2\frac{n_2^{(1)}+n_2^{(2)}}{2}\frac{c}{\varepsilon_\perp\omega}\frac{\partial E_{2x}}{\partial z} - \theta_0(z)\frac{\varepsilon_a}{\varepsilon_\perp}(\cos\varphi_0 E_{2x} + \sin\varphi_0 E_{2y}). \tag{37}$$

C. Light beams in Bragg reflection regime

The Bragg reflection condition is $\lambda = \bar{n}p$, where $\bar{n}$ is the average index of refraction. In this case, the light wavelength falls inside the so called cholesteric gap.[22] In this case, an incident plane polarized beam gives rise only one propagating circularly polarized mode in the cholesteric medium. The second mode, circularly polarized in the opposite direction, lies in the band gap and is evanescent.

We simplify our analysis, assuming strong attenuation of the evanescent mode (i.e., total reflection) and, as in Sec. IV B, neglect effects caused when the propagating mode is reflected from the far side of the cholesteric cell.

To write expressions for propagating waves induced by two incident beams in Bragg reflection regime, we formally may use formulas of previous Subsection IV B, but ignoring the E^+ term in Eqs. (33), (36), and (37).

We obtain expressions for propagating (left polarized) waves omitting in formulas (35) and (36) terms with $e^{i(\omega/c)n_{1,2}^{(2)}(z+L/2)}$ and putting $n_{1,2}^{(1)}$ instead of $\frac{n_{1,2}^{(1)}+n_{1,2}^{(2)}}{2}$ in formulas for $E_{1,2z}$:

$$E_{1x} = \frac{1}{2}A_1 e^{i(\omega/c)n_1^{(1)}(z+L/2)}e^{ik_{1x}x}, E_{1y} = \frac{i}{2}A_1 e^{i(\omega/c)n_1^{(1)}(z+L/2)}e^{ik_{1x}x},$$
$$E_{1z} = i\alpha_1 n_1^{(1)}\frac{c}{\varepsilon_\perp\omega}\frac{\partial E_{1x}}{\partial z} - \theta_0(z)\frac{\varepsilon_a}{\varepsilon_\perp}(\cos\varphi_0 E_{1x} + \sin\varphi_0 E_{1y}), \tag{38}$$

and

$$E_{2x} = \frac{1}{2}A_2 e^{i(\omega/c)n_2^{(1)}(z+L/2)}e^{ik_{2x}x}, E_{2y} = \frac{i}{2}A_2 e^{i(\omega/c)n_2^{(1)}(z+L/2)}e^{ik_{2x}x},$$
$$E_{2z} = -i\alpha_2 n_2^{(1)}\frac{c}{\varepsilon_\perp\omega}\frac{\partial E_{2x}}{\partial z} - \theta_0(z)\frac{\varepsilon_a}{\varepsilon_\perp}(\cos\varphi_0 E_{2x} + \sin\varphi_0 E_{2y}). \tag{39}$$

D. Coupled waves

The coupling between the light waves arises in Eq. (28) as a result of the additional term $\hat{\varepsilon}_3(z)\exp(iqx) + c.c.$ We follow a procedure analogous to that first outlined by Kogelnik,[26] which we have used in our previous related papers.[15,17] The principle involves setting electric field magnitudes $A_1 = A_1(z)$, $A_2 = A_2(z)$, and allowing them to vary slowly across the cell.

We now substitute the electric fields given by Eqs. (35)–(37) (or corresponding expressions for electric fields in Bragg regime) into the wave equation (31). The leading order terms in this substitution cancel because the waves $\mathbf{E}_1$ and $\mathbf{E}_2$ separately obey the vector wave equation with dielectric tensor $\hat{\varepsilon}_1 + \hat{\varepsilon}_2$.

We adopt the undepleted pump approximation,[21] for which the magnitude of the pump beam $|A_2| \gg |A_1|$ and may be regarded as constant. In this case, the set of coupled equations for the electric field magnitudes reduces to (see Eq. (B20) in Appendix B)

$$\frac{\partial}{\partial z}A_1(z) = -iS(z)A_2, \tag{40}$$

where for the wave guide regime

$$S(z) = \frac{\omega}{c}\frac{\varepsilon_a}{n^{(1)}+n^{(2)}}\left[\frac{2\varepsilon_\parallel}{\varepsilon_\perp}\theta(z)\theta_0(z)\cos^2\left[\left(\frac{h}{2}+g\right)\left(z+\frac{L}{2}\right)\right] + \varphi(z)\sin\left[(h+2g)\left(z+\frac{L}{2}\right)\right] + i\alpha h\theta(z)\frac{n^{(1)}+n^{(2)}}{4\varepsilon_\perp}\left\{\sin[g(z+L/2)] - \sin[(h+g)(z+L/2)]\right\}\right], \tag{41}$$

$$h = (\omega/c)(n^{(1)} - n^{(2)}). \tag{41a}$$

For the Bragg reflection regime, the analogous formula is

$$S(z) = \frac{\omega}{c}\frac{\varepsilon_a}{8n^{(1)}}\left[\theta(z)\left\{4\left(1+\frac{\varepsilon_a}{4\varepsilon_\perp}\right)\theta_0(z) - i\alpha\frac{n^{(1)2}}{\varepsilon_\perp}\sin[g(z+L/2)]\right\} - i\alpha\frac{n^{(1)2}}{\varepsilon_\perp}\varphi(z)\theta_0(z)\cos[g(z+L/2)]\right]. \tag{42}$$

The details of the derivation of Eq. (40) have been relegated to Appendix B.

The solution to Eq. (40) has the following form:

$$A_1(z) = A_1(-\mathrm{L}/2) - iA_2\int_{-L/2}^{z} S(z')\,dz'. \tag{43}$$

We now use this solution to investigate energy exchange in the cholesteric cell.

E. Expression for gain coefficient

The signal gain caused by the LC layer in hybrid cell is defined as

$$\Gamma = \frac{A_1(L/2)}{A_1(-L/2)}, \tag{44}$$

where from Eq. (43)

$$A_1(L/2) = A_1(-L/2) - iA_2\int_{-L/2}^{L/2} S(z)\,dz. \tag{45}$$

Substituting $S(z)$ from Eq. (41) into Eq. (45) yields the following result for the signal gain:

$$\Gamma = 1 - i\frac{\omega}{c}\frac{\varepsilon_a}{n^{(1)}+n^{(2)}}\frac{A_2}{A_1(-L/2)}\int_{-L/2}^{L/2} dz\left[2\frac{\varepsilon_\parallel}{\varepsilon_\perp}\theta(z)\theta_0(z)\cos^2\left[\left(\frac{h}{2}+g\right)\left(z+\frac{L}{2}\right)\right] + \varphi(z)\sin\left[(h+2g)\left(z+\frac{L}{2}\right)\right]\right.$$
$$\left. + i\alpha h\theta(z)\frac{n^{(1)}+n^{(2)}}{4\varepsilon_\perp}\left\{\sin[g(z+L/2)] - \sin[(h+g)(z+L/2)]\right\}\right]. \tag{46}$$

Equation (46) can be rewritten, substituting $\theta(z)$ from Eq. (21) and $\varphi(z)$ from Eq. (23). Noting that in the undepleted pump approximation the formula (2) for m reduces to $m \approx 2\cos(2\delta)A_1(-L/2)/A_2$, we obtain

$$\Gamma = 1 + \frac{\omega}{c}\frac{\varepsilon_a}{n^{(1)}+n^{(2)}}\frac{E_{sc}(q)\cos(2\delta)}{q}\int_{-L/2}^{L/2} dz\left[\frac{2\varepsilon_\parallel}{\varepsilon_\perp}\theta_0(z)d(z)\cos^2\left[\left(\frac{h}{2}+g\right)\left(z+\frac{L}{2}\right)\right] + f(z)\sin\left[(h+2g)\left(z+\frac{L}{2}\right)\right]\right.$$
$$\left. + i\alpha hd(z)\frac{n^{(1)}+n^{(2)}}{4\varepsilon_\perp}\left\{\sin[g(z+L/2)] - \sin[(h+g)(z+L/2)]\right\}\right]. \tag{47}$$

The integral in Eq. (47) can now be evaluated, by substituting $d(z)$ from Eq. (22), $f(z)$ from Eq. (24), $\theta_0(z)$ from Eq. (26). We express the result in terms of the exponential gain coefficient:[15,17]

$$g_0 = \frac{1}{L}\ln|\Gamma| = \frac{1}{2L}\ln|(1+a_0A_1\theta_{01})^2 + a_0^2(B_1+C_1)^2|, \tag{48}$$

where

$$a_0 = \frac{\pi}{\lambda}\frac{n_e^2 - n_o^2}{n^{(1)} + n^{(2)}} iE_{sc}(q)\cos(2\delta), \quad A_1 = R_0 R + P,$$
$$B_1 = \frac{r\tilde{q}^2/2}{(\tilde{q}^2 - q^2 - 4g^2)^2 + 16g^2\tilde{q}^2}\left[\frac{\tilde{q}^2 - q^2 - 4g^2 + 4gh}{\tilde{q}^2 + h^2} - \frac{\tilde{q}^2 - q^2 - 20g^2 - 4gh}{\tilde{q}^2 + (4g+h)^2} - \frac{8g(h+2g)}{q^2 + (h+2g)^2}\right], \tag{49}$$
$$C_1 = \left(\frac{\lambda}{4\pi n_e}\right)^2 h\, q\, R_0\left[\frac{A\tilde{q} - (2g+h)B}{\tilde{q}^2 + (2g+h)^2} + \frac{2(h+g)B}{q^2 + g^2 + (h+g)^2} - \frac{A\tilde{q} + hB}{\tilde{q}^2 + h^2} - \frac{A\tilde{q} - 2gB}{\tilde{q}^2 + 4g^2} - \frac{2gB}{q^2 + 2g^2} + \frac{A}{\tilde{q}}\right].$$

Here

$$R_0 = \frac{n_e^2/n_o^2}{(\tilde{q}^2 - q^2 - 2g^2)^2 + 4\tilde{q}^2 g^2}, A = g[r_1(\tilde{q}^2 - q^2 - 2g^2) - 2r\tilde{q}^2], B = \tilde{q}[2r_1 g^2 + r(\tilde{q}^2 - q^2 - 2g^2)],$$
$$R = \frac{2[Ag + B(\tilde{q}+g)]}{(\tilde{q}+g)^2 + g^2} - \frac{2B}{\sqrt{q^2+g^2}+g} + \frac{A(3g+h) + B(\tilde{q}+g)}{(\tilde{q}+g)^2 + (3g+h)^2} - \frac{A(g+h) - B(\tilde{q}+g)}{(\tilde{q}+g)^2 + (g+h)^2} - \frac{2B(\sqrt{q^2+g^2}+g)}{(\sqrt{q^2+g^2}+g)^2 + (2g+h)^2},$$
$$P = \frac{(\tilde{q}+g)(r\tilde{q} - r_1 g)}{(\tilde{q}^2 - q^2 + 2\tilde{q}g)^2 + 4g^2(\tilde{q}+g)^2}\left[\frac{\tilde{q}^2 - q^2 - 6g^2 + 2g(\tilde{q} - h)}{(\tilde{q}+g)^2 + (h+3g)^2} - \frac{\tilde{q}^2 - q^2 + 2g^2 + 2g(\tilde{q}+h)}{(\tilde{q}+g)^2 + (h+g)^2} + \frac{4g(h+2g)}{q^2 + (h+2g)^2}\right]. \tag{50}$$

When the incident light wavelength lies in the cholesteric gap, we substitute in Eq. (45) expressions (42). In this case, the exponential gain coefficient is described by the expression

$$g_0 = \frac{1}{L}\ln|1 + a_0 B_2(A_2\theta_{01} + C_2)|, \tag{51}$$

where in Eq. (51)

$$A_2 = \frac{n_e^2 + 3n_o^2}{4n_o^2}\left[\frac{Ag + (\tilde{q}+g)B}{(\tilde{q}+g)^2 + g^2} - \frac{B}{(g + \sqrt{q^2+g^2})}\right]$$
$$B_2 = \frac{1}{(\tilde{q}^2 - q^2 - 2g^2)^2 + 4\tilde{q}^2 g^2},$$
$$C_2 = \frac{\lambda}{4\pi}\frac{n^{(1)}}{8n_0^2} q\left[\frac{2gA + \tilde{q}B}{\tilde{q}^2 + 4g^2} - \frac{2gA}{q^2 + 2g^2} - \frac{B}{\tilde{q}}\right]. \tag{52}$$

F. Generalization of q-dependence in nonlinear theory

In Ref. 15, we have developed a theory for two beam energy exchange in hybrid nematic cells. The gain coefficient g_0 contains a phenomenological multiplier nonlinear in the photorefractive electric field magnitude $E_{sc}(q)$. We have suggested that this multiplier takes the form $E_{sc}(q)\left(1 + \mu(L,q)E_{sc}^2(q)\right)$, and thus at small director grating spacing (high q) $\mu(L,q) \approx \mu(L)q^2$. If $\mu(L)$ is taken as a fitting parameter, these forms are consistent with the experimental dependence of gain coefficient on grating spacing in hybrid nematic LC,[15] as well as with experimental results in a hybrid cholesteric LC relating to thin cells in a dual photorefractive window geometry.[17] In Ref. 15, we discussed different physical mechanisms responsible for the nonlinear dependence of the gain coefficient on $E_{sc}(q)$, identifying the physical separation of LC components with different molecular dipoles as the probably principal physical contribution.

As already noted in Sec. I, the theoretical gain coefficient with this form of $\mu(L,q)$ fails to describe those experimental results obtained in a one window geometry. We hypothesize that this is connected with the form of the multiplier $\mu(L,q) \approx \mu(L)q^2$, which inaccurately describes the large grating spacing (low q) regime. In Appendix C, we analyze the q-dependence of this nonlinear multiplier in the cholesteric cell.

As a result, accounting for a change of spatial distribution of dipole concentration in cholesteric cell we have to replace in Eqs. (21)–(26) for director angles and in Eqs. (49), (50), and (52) for gain coefficient, the flexoelectric parameters r, r_1 (denoting here as r_i) by their effective values

$$r_i = r_i^0\left[1 + \mu\left(q + \frac{\mu_1}{q}\right)^2 |E_{sc}|^2\right], \tag{53}$$

where r_i^0 are the flexoelectric parameters in the absence of photorefractive field, and μ and μ_1 are the fitting parameters.

V. COMPARISON WITH EXPERIMENTAL DATA

In this section, we compare our theoretical results (Subsections IV E and IV F) with experimental data for a single photorefractive window hybrid cell obtained by Cook *et al.*[16] The theory presents results for the dependence of the exponential gain coefficient on grating spacing, We recall that in the experiments,[16] the hybrid cell was filled with cholesteric mixture by doping the nematic LC BL038 with the chiral impurity CB15. The LC BC038 is a proprietary material prepared by the Merck company (EMD Millipore in North America), which contains seven components including some cyanobiphenyl derivatives, one of which is 5CB.[28] CB15 is a widely used right-handed chiral agent also available from Merck-EMD Millipore.

In order to evaluate $E_{sc}(q)$, we follow the formulas (5) and the paper of Cook *et al.*[10] Here, the ratio of the acceptor to donor impurity densities is estimated to be very small, i.e.,

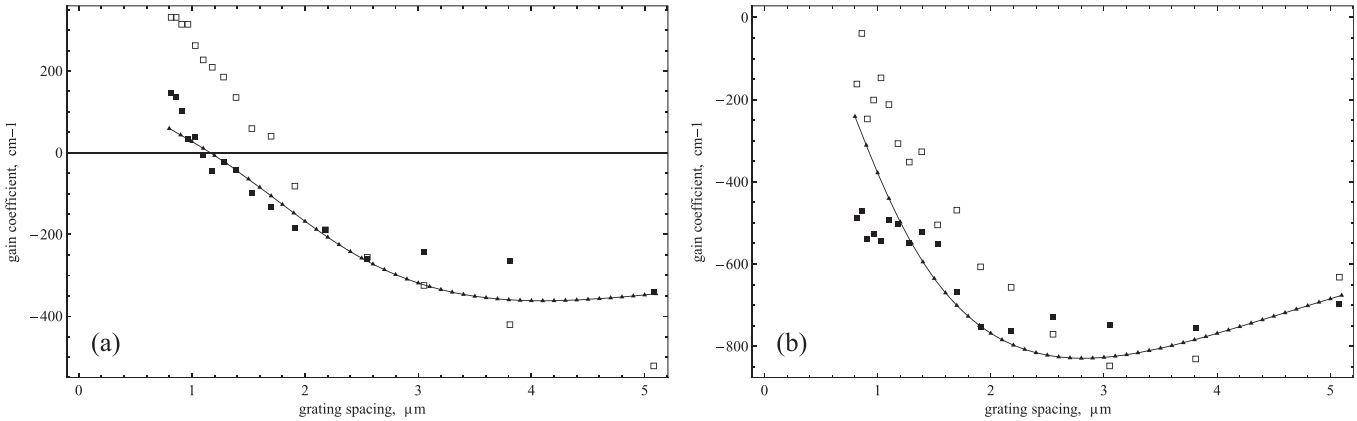

FIG. 3. Gain coefficient g_0 versus grating spacing Λ in hybrid cell containing cholesteric LC mixture BL038/CB15. Theoretical results—curves, experimental data—boxes. $\lambda = 0.532\,\mu$m (a) above cholesteric gap, notch position $\lambda_0 = 440$ nm; (b); below cholesteric gap, notch position $\lambda_0 = 650$ nm. Note: the black and white boxes correspond to two different cells, with experiments carried out at different times. The results of the two sets of experiments are consistent, showing that the data are reproducible, apart from errors due to minor differences in experimental preparation conditions.

$N_d \gg N_a$, with $N_a \approx 3.8 \times 10^{21}\,\mathrm{m}^{-3}$. The director pretilt angle at the LC cell substrates was approximately 12°, yielding $\theta_{01} = 12^\circ$, $\theta_{02} = -12^\circ$. The ordinary and extraordinary refractive indices of the mixture BL038/CB15 are $n_o = 1.527$ and $n_e = 1.799$, respectively, with low-frequency dielectric constants $\tilde{\varepsilon}_{\|} = 21.7$ and $\tilde{\varepsilon}_{\perp} = 5.3$. The dielectric permittivity of the photorefractive layers is given by $\varepsilon_{Ph} = 200$ at temperature $T = 300$ K.

The ratios of flexoelectric to elastic moduli in the absence of photorefractive field $r^0 = (e_1 + e_3)/K$ and $r_1^0 = (e_1 - e_3)/K$ are not known for BL038/CB15. But these ratios have been measured in other LC systems,[29–32] and a value of order of magnitude $\sim 1\,\mathrm{Cm}^{-1}\mathrm{N}^{-1}$ may be regarded as typical for absolute values of r_0 and r_1^0 (note that $r_1^0 < 0$). We describe effective values of the flexoelectric parameters using Eq. (53), where we evaluate the fitting parameter $\mu = 8 \times 10^{-20}\,\mathrm{J}^{-2}\,\mathrm{C}^2\,\mathrm{m}^4$. This value of μ was obtained in our earlier paper[17] when fitting the experimental curves for beam coupling in a cell with same cholesteric mixture, but in the different dual photorefractive window geometry. Thus, to fit experimental curves for the single photorefractive window geometry, we need only the one extra fitting parameter μ_1 in Eq. (53).

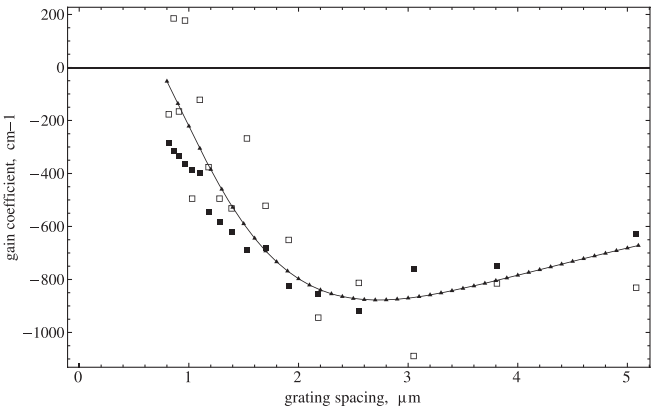

FIG. 4. Gain coefficient g_0 versus grating spacing Λ in hybrid cell containing cholesteric LC mixture BL038/CB15. Experimental data—boxes. Light wavelength inside the cholesteric gap; notch position $\lambda_0 = 532$ nm. Black and white boxes correspond to different experiments on different cells, as discussed in Fig. 3 caption.

We note here some details of the experimental data from Ref. 16, to which we are fitting our theory. The laser wave length has $\lambda = 532$ nm. The gap is localized by the notch position (at which there is a decrease in the light transmission). In the two cases considered, the notches occur at $\lambda_0 = 440$ nm and at $\lambda_0 = 650$ nm. The formula for the notch width is $\Delta\lambda = \Delta n\, p = \lambda_0 \frac{\Delta n}{n}$,[33] where p is the cholesteric pitch. In the two experimentally relevant cases, this corresponds, respectively, to $\Delta\lambda = 86$ nm and $\Delta\lambda = 120$ nm, which means that the notches are in the range (440 ± 43)nm and (650 ± 60)nm. Thus, in the first case, the gap is well below the wavelength of the incident light, and in the second case it is well above the light wavelength.

In Figs. 3 and 4, the gain coefficient g_0 versus the grating spacing $\Lambda = 2\pi/q$ is plotted for cells of thickness $L = 5\,\mu$m. In Fig. 3, results are presented for cases in which the incident light wavelength is above (Fig. 3(a)), as well as below (Fig. 3(b)), the cholesteric gap. Fig. 4 shows the case when light wavelength is inside the cholesteric gap. The best fit of theoretical curves (48) in Fig. 3 and (51) in Fig. 4 with experimental data occurs for absolute values of parameters r^0, r_1^0 from the range $1 - 4 (r^0 > 0,\ r_1^0 < 0)$. In all cases, the value of fitting parameter μ_1 was the same and equal to $\mu_1 = 1.3 \times 10^{13}\,\mathrm{m}^{-2}$.

For light beam wavelengths outside the cholesteric gap, an additional fitting parameter exists, namely, the difference between the refraction indices associated with the left-handed and right-handed circular polarized light waves, $\Delta n = n^{(1)} - n^{(2)}$. This parameter characterizes the optical rotation in the cholesteric LC. In both cases, above and below the cholesteric gap, the value of this parameter did not exceed 10^{-3}. This corresponds to a numerical value for the optical rotation of the light beam passing through the cell equal to $\frac{2\pi}{\lambda}\Delta n\, L \approx 3.5^\circ$, and is consistent with earlier experimental results,[16] in which in a similar experimental setup, there appeared to be no noticeable change in the light beam polarization.

VI. CONCLUSIONS

We have developed a theoretical model describing energy gain of a weak signal beam interacting with a strong

pump beam at a diffraction grating in a hybrid photorefractive-cholesteric cell. The grating is written on the director of the cholesteric LC cell by the space-charge field induced by interfering light beams in the photorefractive substrate which penetrate into the LC. The model includes the fact that, in these systems, flexoelectric electric field-director coupling is more important than LC static dielectric anisotropy coupling.

Each beam induces two circular polarized waves propagating in the cholesteric across the cell, with different velocities. The model thus also includes optical rotation in the cholesteric LC. We have studied cases when the wavelength of incident plane polarized light beams falls above, below or inside the cholesteric gap. In the last case, only a single circular polarized wave propagates across the cholesteric cell.

In hybrid cells filled with cholesteric mixtures BL038/CB15, a consistent explanation of the experimental results also requires the inclusion of an extra multiplier in the magnitude of the director grating. This multiplier is non-linear in the photorefractive electric field. We have been able to justify, at least in principle, the q-dependence of the non-linear multiplier, but this part of the model requires further justification in terms of microscopic physics. We have then calculated two-beam energy exchange, subject to a small number of fitting parameters. Our theoretical curves describe well experimental data for gain coefficient versus grating spacing in all cholesteric mixtures used in a single window geometry.

Finally, we pose the question of other applications of this theory, which might at the same time subject the theory to a more severe experimental test. We note first the existence of chiral dopants which are widely tunable with UV light.[34] Using such a dopant, in the same cell, one could in principle tune the cholesteric gap through the wavelength of the ambient laser light. In this system, the beam coupling would be observed to change as a function of the intensity of the imposed UV irradiation. This system would be one for which the present theory should be applicable. It would only be necessary theoretically to establish the fitting parameters at one value of the chirality. Thus, the theory would be subject to an unambiguous test.

A second application might use an aligning layer with tunable anchoring; this could in principle be either the anchoring energy or the director pretilt.[35] By utilizing this type of aligning, one could check how the beam coupling is sensitive to the anchoring. Finally, we raise the possibility of using an inhomogeneous cholesteric, in which there exists a pitch gradient.[36] In this case, it is possible that the initial pitch gradient may result in an initially nonzero flexopolarization, which is not the case for a cholesteric with a homogeneous spiral. We have elsewhere speculated that the flexopolarisation is an important factor in the LC director reorientation.[15] Hence, altering the initial flexopolarization may increase the cell sensitivity to the space-charge field.

ACKNOWLEDGMENTS

This work has been partially supported by EOARD Grant 078001(V.Y.R. and I.P.P.). I.P.P. and T.J.S. thank the Isaac Newton Institute for Mathematical Sciences, Cambridge, UK, for hospitality during the preparation of this manuscript.

APPENDIX A: EQUATIONS FOR THE ELECTRIC FIELD FOR OBLIQUELY INCIDENT LIGHT BEAMS

Let the cholesteric LC dielectric tensor be $\hat{\varepsilon}(z) = \hat{\varepsilon}_1(z) + \hat{\varepsilon}_2(z)$. A light beam polarized in the xz-plane is incident on the cell, with small angle of incidence α with respect to the cell normal (the z-axis). In the cholesteric LC cell under consideration, the light beam electric vector depends on coordinates x, z, and satisfies the wave equation

$$\nabla \times \nabla \times \mathbf{E}(x,z) - \frac{\omega^2}{c^2}\hat{\varepsilon}(\mathrm{z})\mathbf{E}(x,z) = 0. \qquad \text{(A1)}$$

We note that

$$\nabla \times \nabla \times \mathbf{E} = \nabla \times \begin{vmatrix} \boldsymbol{i} & \boldsymbol{j} & \boldsymbol{k} \\ \frac{\partial}{\partial x} & \frac{\partial}{\partial y} & \frac{\partial}{\partial z} \\ E_x(x,z) & E_y(x,z) & E_z(x,z) \end{vmatrix} = \nabla \times \left[-\boldsymbol{i}\frac{\partial}{\partial z}E_y - \boldsymbol{j}\left(\frac{\partial}{\partial x}E_z - \frac{\partial}{\partial z}E_x\right) + \boldsymbol{k}\frac{\partial}{\partial x}E_y \right]$$

$$= \begin{vmatrix} \boldsymbol{i} & \boldsymbol{j} & \boldsymbol{k} \\ \frac{\partial}{\partial x} & \frac{\partial}{\partial y} & \frac{\partial}{\partial z} \\ -\frac{\partial}{\partial z}E_y & -\left(\frac{\partial}{\partial x}E_z - \frac{\partial}{\partial z}E_x\right) & \frac{\partial}{\partial x}E_y \end{vmatrix} = \boldsymbol{i}\frac{\partial}{\partial z}\left(\frac{\partial}{\partial x}E_z - \frac{\partial}{\partial z}E_x\right) - \boldsymbol{j}\left(\frac{\partial^2}{\partial x^2}E_y + \frac{\partial^2}{\partial z^2}E_y\right)$$

$$- \boldsymbol{k}\frac{\partial}{\partial x}\left(\frac{\partial}{\partial x}E_z - \frac{\partial}{\partial z}E_x\right) = \boldsymbol{i}\left(\frac{\partial^2}{\partial z \partial x}E_z - \frac{\partial^2}{\partial z^2}E_x\right) - \boldsymbol{j}\left(\frac{\partial^2}{\partial x^2} + \frac{\partial^2}{\partial z^2}\right)E_y - \boldsymbol{k}\left(\frac{\partial^2}{\partial x^2}E_z - \frac{\partial^2}{\partial x \partial z}E_x\right).$$

Thus, the wave equation (A1) takes the form

$$\frac{\partial^2 E_x}{\partial z^2} - \frac{\partial^2 E_z}{\partial z \partial x} + \frac{\omega^2}{c^2}\varepsilon_{xi}(z)E_i = 0\,,$$
$$\frac{\partial^2 E_y}{\partial x^2} + \frac{\partial^2 E_y}{\partial z^2} + \frac{\omega^2}{c^2}\varepsilon_{yi}(z)E_i = 0\,, \tag{A2}$$
$$\frac{\partial^2 E_z}{\partial x^2} - \frac{\partial^2 E_x}{\partial z \partial x} + \frac{\omega^2}{c^2}\varepsilon_{zi}(z)E_i = 0\,.$$

We seek a solution to the system of Eqs. (A2), in the form

$$\boldsymbol{E} = \boldsymbol{A}_0 \exp[i(\boldsymbol{k}\cdot\boldsymbol{r} - \omega t)], \tag{A3}$$

where wave vector $\boldsymbol{k} = k(\sin\alpha, 0, \cos\alpha)$. The terms $\frac{\partial^2 E_{y,z}}{\partial x^2}$ in Eqs. (A2) are proportional to the square of small angle α and can be neglected. The system of Eqs. (A2) then reduces to

$$\frac{\partial^2 E_x}{\partial z^2} - \frac{\partial^2 E_z}{\partial z \partial x} + \frac{\omega^2}{c^2}\varepsilon_{xi}(z)E_i = 0\,,$$
$$\frac{\partial^2 E_y}{\partial z^2} + \frac{\omega^2}{c^2}\varepsilon_{yi}(z)E_i = 0\,, \tag{A4}$$
$$-\frac{\partial^2 E_x}{\partial z \partial x} + \frac{\omega^2}{c^2}\varepsilon_{zi}(z)E_i = 0\,.$$

Using Eq. (29) for $\hat{\varepsilon}(z) = \hat{\varepsilon}_1(z) + \hat{\varepsilon}_2(z)$), we can linearize Eqs. (A4) with respect to small angles α,θ_0, yielding

$$\frac{\partial^2}{\partial z^2}\begin{pmatrix} E_x \\ E_y \end{pmatrix} - \frac{\partial^2}{\partial z \partial x}\begin{pmatrix} E_z \\ 0 \end{pmatrix} + \frac{\omega^2}{c^2}\begin{pmatrix} \varepsilon_\perp + \varepsilon_a \cos^2\varphi_0 & \frac{1}{2}\varepsilon_a \sin 2\varphi_0 \\ \frac{1}{2}\varepsilon_a \sin 2\varphi_0 & \varepsilon_\perp + \varepsilon_a \sin^2\varphi_0 \end{pmatrix}\begin{pmatrix} E_x \\ E_y \end{pmatrix} + \varepsilon_a\theta_0\frac{\omega^2}{c^2}\begin{pmatrix} \cos\varphi_0 \\ \sin\varphi_0 \end{pmatrix}E_z = 0$$
$$-\frac{\partial^2 E_x}{\partial z \partial x} + \frac{\omega^2}{c^2}[\varepsilon_a\theta_0(\cos\varphi_0 E_x + \sin\varphi_0 E_y) + \varepsilon_\perp E_z] = 0. \tag{A5}$$

Equation (A5) yields an expression for the z-component of the electric vector:

$$E_z = \frac{c^2}{\varepsilon_\perp \omega^2}\frac{\partial^2 E_x}{\partial z \partial x} - \theta_0\frac{\varepsilon_a}{\varepsilon_\perp}(\cos\varphi_0 E_x + \sin\varphi_0)E_y. \tag{A6}$$

Substituting (A6) into Eq. (A5), and neglecting second order terms in the small quantities α,θ_0, we obtain

$$\frac{\partial^2}{\partial z^2}\begin{pmatrix} E_x \\ E_y \end{pmatrix} + \frac{\omega^2}{c^2}\begin{pmatrix} \varepsilon_\perp + \varepsilon_a \cos^2\varphi_0 & \frac{1}{2}\varepsilon_a \sin 2\varphi_0 \\ \frac{1}{2}\varepsilon_a \sin 2\varphi_0 & \varepsilon_\perp + \varepsilon_a \sin^2\varphi_0 \end{pmatrix}\begin{pmatrix} E_x \\ E_y \end{pmatrix} = 0. \tag{A7}$$

Equation (A7) coincides with those for a light beam normally incident on the cholesteric LC cell,[22] which have already been obtained. In order to obtain the solution to Eq. (A6), it then only necessary to substitute into Eq. (A6) for the z-component of electric vector.

APPENDIX B: EQUATIONS FOR SIGNAL BEAM AMPLITUDE IN SLOWLY VARYING AMPLITUDE APPROXIMATION

Two intersecting light beams propagate in the cholesteric LC cell with a director grating: a small signal beam with amplitude A_1 and a strong pump beam with amplitude A_2. The director grating induces a spatially modulation of the dielectric tensor of cholesteric cell (see Eq. (28)), which in turn couples the light beams. We here obtain equations for the amplitudes of the light beams as a function of position. This permits an analysis of the effect of the director grating parameters on the beam-coupling and hence on the amplitude of the signal beam.

The electric field vector of the beams satisfies Eq. (31) with dielectric tensor (28) and has a form described by Eqs. (35)–(37). To solve Eq. (31), we first consider the wave equation in a cholesteric LC characterized by a dielectric tensor $\hat{\varepsilon}_1+\hat{\varepsilon}_2$ (see Eq. (29)) that does not contain a spatially modulated term. In this case, the wave equation for the electric vector of both light beams $\mathbf{E} = \mathbf{E_1} + \mathbf{E_2}$ takes the form:

$$\nabla\times\nabla\times\ \mathbf{E} - \frac{\omega^2}{c^2}(\hat{\varepsilon}_1+\hat{\varepsilon}_2)\mathbf{E} = 0. \tag{B1}$$

Equation (B1) can be decomposed into equations for the light vector of each beam

$$\nabla\times\nabla\times\ \mathbf{E_1} - \frac{\omega^2}{c^2}(\hat{\varepsilon}_1+\hat{\varepsilon}_2)\mathbf{E_1} = 0,$$
$$\nabla\times\nabla\times\ \mathbf{E_2} - \frac{\omega^2}{c^2}(\hat{\varepsilon}_1+\hat{\varepsilon}_2)\mathbf{E_2} = 0, \tag{B2}$$

where $\mathbf{E_1}$ and $\mathbf{E_2}$ are defined by Eqs. (36) and (37) and possess constant amplitudes A_1 and A_2, respectively.

In a cholesteric LC, characterized by a dielectric tensor with periodic modulation $\hat{\varepsilon}_1+\hat{\varepsilon}_2+\left[\hat{\varepsilon}_3(z)\exp(iqx) + c.c.\right]$ (see Eq. (28)), the light beam electric vector $\tilde{\mathbf{E}}$ satisfies the modified equation:

$$\nabla\times\nabla\times\ \tilde{\mathbf{E}} - \frac{\omega^2}{c^2}(\hat{\varepsilon}_1+\hat{\varepsilon}_2+[\hat{\varepsilon}_3\exp(iqx) + c.c.])\tilde{\mathbf{E}} = 0. \tag{B3}$$

We now seek a solution to Eq. (B3) in the form

$$\tilde{\mathbf{E}} = \frac{A_1(z)}{A_1}\mathbf{E_1} + \frac{A_2(z)}{A_2}\mathbf{E_2}, \tag{B4}$$

in which the amplitude of the electric vector of each beam is now z-dependent.

Combining Eqs. (B3) and (B4), we now obtain

$$\nabla\times\nabla\times\left[\frac{A_1(z)}{A_1}\mathbf{E_1}+\frac{A_2(z)}{A_2}\mathbf{E_2}\right]-\frac{\omega^2}{c^2}(\hat{\varepsilon}_1+\hat{\varepsilon}_2 +[\hat{\varepsilon}_3\exp(\mathrm{iqx})+c.\mathrm{c.}])\left[\frac{A_1(z)}{A_1}\mathbf{E_1}+\frac{A_2(z)}{A_2}\mathbf{E_2}\right]=0\,. \quad \text{(B5)}$$

A solution for Eq. (B5) can be found in the limit in which $A_1(z)$ and $A_2(z)$ are weakly dependent on z. This involves omitting second derivatives of $A_1(z)$ and $A_2(z)$ in Eq. (B5), yielding

$$\begin{aligned}&\nabla\frac{A_1(z)}{A_1}\nabla\cdot\mathbf{E_1}+\frac{A_1(z)}{A_1}\nabla(\nabla\cdot\mathbf{E_1})+\nabla E_{1z}\frac{\partial}{\partial z}\frac{A_1(z)}{A_1}+\nabla\frac{A_2(z)}{A_2}\nabla\cdot\mathbf{E_2}+\frac{A_2(z)}{A_2}\nabla(\nabla\cdot\mathbf{E_2})\\&+\nabla E_{2z}\frac{\partial}{\partial z}\frac{A_2(z)}{A_2}-2\left[\frac{\partial}{\partial z}\frac{A_1(z)}{A_1}\frac{\partial}{\partial z}\mathbf{E_1}+\frac{\partial}{\partial z}\frac{A_2(z)}{A_2}\frac{\partial}{\partial z}\mathbf{E_2}\right]-\left[\frac{A_1(z)}{A_1}\nabla^2\mathbf{E_1}+\frac{A_2(z)}{A_2}\nabla^2\mathbf{E_2}\right]\\&-\frac{\omega^2}{c^2}(\hat{\varepsilon}_1+\hat{\varepsilon}_2+[\hat{\varepsilon}_3\exp(iqx)+c.c.])\left[\frac{A_1(z)}{A_1}\mathbf{E_1}+\frac{A_2(z)}{A_2}\mathbf{E_2}\right]=0\,.\end{aligned} \quad \text{(B6)}$$

Combining Eqs. (B2) and (B6) now yields

$$\begin{aligned}&\nabla\frac{A_1(z)}{A_1}\nabla\cdot\mathbf{E_1}+\nabla E_{1z}\frac{\partial}{\partial z}\frac{A_1(z)}{A_1}+\nabla\frac{A_2(z)}{A_2}\nabla\cdot\mathbf{E_2}+\nabla E_{2z}\frac{\partial}{\partial z}\frac{A_2(z)}{A_2}\\&-2\left[\frac{\partial}{\partial z}\frac{A_1(z)}{A_1}\frac{\partial}{\partial z}\mathbf{E_1}+\frac{\partial}{\partial z}\frac{A_2(z)}{A_2}\frac{\partial}{\partial z}\mathbf{E_2}\right]-\frac{\omega^2}{c^2}[\hat{\varepsilon}_3\exp(iqx)+c.c.]\left[\frac{A_1(z)}{A_1}\mathbf{E_1}+\frac{A_2(z)}{A_2}\mathbf{E_2}\right]=0\,.\end{aligned} \quad \text{(B7)}$$

After some algebra, we obtain the following equation:

$$(\mathbf{k}\nabla\cdot\mathbf{E_1}+\nabla E_{1z}-2\frac{\partial}{\partial z}\mathbf{E_1})\frac{\partial}{\partial z}\frac{A_1(z)}{A_1}+\left(\mathbf{k}\nabla\cdot\mathbf{E_2}+\nabla E_{2z}-2\frac{\partial}{\partial z}\mathbf{E_2}\right)\frac{\partial}{\partial z}\frac{A_2(z)}{A_2}=\frac{\omega^2}{c^2}[\hat{\varepsilon}_3\exp(iqx)+c.c.]\left[\frac{A_1(z)}{A_1}\mathbf{E_1}+\frac{A_2(z)}{A_2}\mathbf{E_2}\right], \quad \text{(B8)}$$

where $\mathbf{k}$ is a unit Cartesian vector. Now, recalling that $q=k_{1\mathrm{x}}-k_{2\mathrm{x}}$, $\mathbf{E_1}\sim\exp(ik_{1x}x)$, $\mathbf{E_2}\sim\exp(ik_{2x}x)$, we collect terms with the same exponents $\exp(ik_{1\mathrm{x}}x)$ and $\exp(ik_{2\mathrm{x}}x)$ in Eq. (B8). This identifies the following system of two coupled equations:

$$(\mathbf{k}\nabla\cdot\mathbf{E_1}+\nabla E_{1z}-2\frac{\partial}{\partial z}\mathbf{E_1})\frac{\partial}{\partial z}\frac{A_1(z)}{A_1}=\frac{\omega^2}{c^2}\hat{\varepsilon}_3\mathrm{e}^{iqx}\mathbf{E_2}\frac{A_2(z)}{A_2}, \quad \text{(B9)}$$

$$(\mathbf{k}\nabla\cdot\mathbf{E_2}+\nabla E_{2z}-2\frac{\partial}{\partial z}\mathbf{E_2})\frac{\partial}{\partial z}\frac{A_2(z)}{A_2}=\frac{\omega^2}{c^2}\hat{\varepsilon}_3^*\mathrm{e}^{-iqx}\mathbf{E_1}\frac{A_1(z)}{A_1}. \quad \text{(B10)}$$

Further, recalling Eqs. (36) and (37)

$$\nabla\cdot\mathbf{E_{1,2}}=ik_{1,2x}E_{1,2x}+\frac{\partial}{\partial z}E_{1,2z},$$
$$\nabla E_{1,2z}=ik_{1x}\mathbf{i}E_{1,2z}+\mathbf{k}\frac{\partial}{\partial z}E_{1,2z},$$

Eqs. (B9) and (B10) can now be rewritten as

$$[ik_{1x}\mathbf{k}E_{1x}+ik_{1x}\boldsymbol{i}E_{1z}-2\frac{\partial}{\partial z}(\mathbf{i}E_{1x}+\mathbf{j}E_{1y})]\frac{\partial}{\partial z}\frac{A_1(z)}{A_1} =\frac{\omega^2}{c^2}\hat{\varepsilon}_3\mathrm{e}^{iqx}\mathbf{E_2}\frac{A_2(z)}{A_2}, \quad \text{(B11)}$$

$$\left[ik_{2x}\mathbf{k}E_{2x}+ik_{2x}\boldsymbol{i}E_{2z}-2\frac{\partial}{\partial z}(\mathbf{i}E_{2x}+\mathbf{j}E_{2y})\right]\frac{\partial}{\partial z}\frac{A_2(z)}{A_2} =\frac{\omega^2}{c^2}\hat{\varepsilon}_3^*\mathrm{e}^{-iqx}\mathbf{E_1}\frac{A_1(z)}{A_1}. \quad \text{(B12)}$$

Left-multiplying both sides of Eq. (B11) by $\mathbf{E_1^*}$, and of Eq. (B12) by $\mathbf{E_2^*}$ yields

$$\left[ik_{1x}(E_{1x}E_{1z}^*+E_{1x}^*E_{1z})-2\left(E_{1x}^*\frac{\partial}{\partial z}E_{1x}+E_{1y}^*\frac{\partial}{\partial z}E_{1y}\right)\right]\times\frac{\partial}{\partial z}\frac{A_1(z)}{A_1}=\frac{\omega^2}{c^2}\mathbf{E_1^*}\hat{\varepsilon}_3\mathbf{E_2}\mathrm{e}^{iqx}\frac{A_2(z)}{A_2}, \quad \text{(B13)}$$

$$\left[ik_{2x}(E_{2z}^*E_{2x}+E_{2x}^*E_{2z})-2\left(E_{2x}^*\frac{\partial}{\partial z}E_{2x}+E_{2y}^*\frac{\partial}{\partial z}E_{2y}\right)\right]\times\frac{\partial}{\partial z}\frac{A_2(z)}{A_2}=\frac{\omega^2}{c^2}\mathbf{E_2^*}\hat{\varepsilon}_3^*\mathbf{E_1}\mathrm{e}^{-iqx}\frac{A_1(z)}{A_1}. \quad \text{(B14)}$$

Equations (B13) and (B14) can now be examined, isolating leading order terms in the small angles α and θ_0. The left-hand terms in the square brackets are now second order in the small angles α,θ_0 and can be omitted, yielding the following set of coupled equations:

$$\left(E_{1x}^*\frac{\partial}{\partial z}E_{1x}+E_{1y}^*\frac{\partial}{\partial z}E_{1y}\right)\frac{\partial}{\partial z}\frac{A_1(z)}{A_1}=-\frac{\omega^2}{2c^2}\mathbf{E_1^*}\hat{\varepsilon}_3\mathbf{E_2}\mathrm{e}^{iqx}\frac{A_2(z)}{A_2}, \quad \text{(B15)}$$

$$\left(E_{2x}^{*}\frac{\partial}{\partial z}E_{2x}+E_{2y}^{*}\frac{\partial}{\partial z}E_{2y}\right)\frac{\partial}{\partial z}\frac{A_2(z)}{A_2}=-\frac{\omega^2}{2c^2}\mathbf{E_2}^{*}\hat{\varepsilon}_3^{*}\mathbf{E_1}e^{-iqx}\frac{A_1(z)}{A_1}. \tag{B16}$$

We now recall that beam 1 is the signal and beam 2 is the pump, with the consequence that the pump magnitude $|A_2| \gg |A_1|$. In the undepleted pump approximation,[21] the signal has a negligible effect on the pump amplitude, which may consequently be regarded as constant, $A_2(z) = A_2$. In this case, the set of coupled Eqs. (B15)–(B16) reduces to the single equation

$$\left(E_{1x}^{*}\frac{\partial}{\partial z}E_{1x}+E_{1y}^{*}\frac{\partial}{\partial z}E_{1y}\right)\frac{\partial}{\partial z}\frac{A_1(z)}{A_1}=-\frac{\omega^2}{2c^2}\mathbf{E_1}^{*}\hat{\varepsilon}_3\mathbf{E_2}e^{iqx}. \tag{B17}$$

We now discuss the case in which the wave vectors of the light beams are symmetric with regard to the cell normal, so that the incidence angles are equal, $\alpha_1 = \alpha_2 \equiv \alpha$. Since the angle α is small, the refractive indices for waves with the same circular polarization may be regarded as equal, $n_1^{(1)} = n_2^{(1)} = n^{(1)}$, $n_1^{(2)} = n_2^{(2)} = n^{(2)}$. We define $h = (\omega/c)(n^{(1)} - n^{(2)})$.

Now suppose that the conditions are such that the wave guide regime (Sec. IV B) applies. Then, using Eqs. (35) and (36) for $\mathbf{E_1}$, $\mathbf{E_2}$ and Eq. (30) for $\hat{\varepsilon}_3$ we can calculate expressions in left and right sides of Eq. (B17)

$$E_{1x}^{*}\frac{\partial}{\partial z}E_{1x}+E_{1y}^{*}\frac{\partial}{\partial z}E_{1y}=2i(\omega/c)\left(\frac{A_1}{2}\right)^2(n^{(1)}+n^{(2)}), \tag{B18}$$

$$\mathbf{E_1}^{*}\hat{\varepsilon}_3\mathbf{E_2}e^{iqx}=-A_1A_2\varepsilon_a\left\{\varphi(z)\sin\left[(h+2g)\left(z+\frac{L}{2}\right)\right]+2\theta(z)\left[\theta_0(z)\left(1+\frac{\varepsilon_a}{\varepsilon_\perp}\right)\cos^2\left[\left(\frac{h}{2}+g\right)\left(z+\frac{L}{2}\right)\right]+i\alpha\frac{n^{(1)2}-n^{(2)2}}{8\varepsilon_\perp}\right.\right.$$
$$\left.\left.\times\left\{\sin\varphi_0-\sin\left[(h+g)\left(z+\frac{L}{2}\right)\right]\right\}\right]\right\}. \tag{B19}$$

Substituting Eqs. (B18) and (B19) into Eq. (B17), we obtain the following equation for the signal beam amplitude:

$$\frac{\partial A_1(z)}{\partial z}=-i\frac{\omega}{c}\frac{\varepsilon_a}{n^{(1)}+n^{(2)}}\left[2\frac{\varepsilon_\parallel}{\varepsilon_\perp}\theta(z)\theta_0(z)\cos^2\left[\left(\frac{h}{2}+g\right)\left(z+\frac{L}{2}\right)\right]+i\alpha\frac{n_1^{(1)2}-n_1^{(2)2}}{4\varepsilon_\perp}\theta(z)\right.$$
$$\left.\times\left\{\sin[g(z+L/2)]-\sin[(h+g)(z+L/2)]\right\}+\varphi(z)\sin\left[(h+2g)\left(z+\frac{L}{2}\right)\right]\right]A_2\,. \tag{B20}$$

Now we can use Eq. (B20) to calculate amplitude of the signal beam in the wave guide regime (see Subsections IV D and IV E).

On the other hand, in the Bragg reflection regime, analogous calculations yield

$$E_{1x}^{*}\frac{\partial}{\partial z}E_{1x}+E_{1y}^{*}\frac{\partial}{\partial z}E_{1y}=2i(\omega/c)\left(\frac{A_1}{2}\right)^2 n^{(1)}, \tag{B21}$$

$$\mathbf{E_1}^{*}\hat{\varepsilon}_3\mathbf{E_2}e^{iqx}=\frac{1}{8}\varepsilon_aA_1A_2\left\{\theta(z)\left[-4\theta_0(z)\left(1+\frac{\varepsilon_a}{4\varepsilon_\perp}\right)+i\alpha\frac{n^{(1)2}}{\varepsilon_\perp}\sin[g(z+L/2)]\right]+i\alpha\frac{n^{(1)2}}{\varepsilon_\perp}\varphi(z)\theta_0(z)\cos[g(z+L/2)]\right\}. \tag{B22}$$

Substituting Eqs. (B21), (B22) into Eq. (B17) yields the following equation for the amplitude in the Bragg regime:

$$\frac{\partial}{\partial z}A_1(z)=-i\frac{\omega}{c}\frac{\varepsilon_a}{8n^{(1)}}\left\{\theta(z)\left[4\left(1+\frac{\varepsilon_a}{4\varepsilon_\perp}\right)\theta_0(z)-i\alpha\frac{n^{(1)2}}{\varepsilon_\perp}\sin[g(z+L/2)]\right]-i\alpha\frac{n^{(1)2}}{\varepsilon_\perp}\varphi(z)\theta_0(z)\cos[g(z+L/2)]\right\}A_2. \tag{B23}$$

The solution to Eq. (B23) enables the signal beam amplitude in the Bragg regime (Subsections IV D and IV E) to be obtained.

APPENDIX C. ESTIMATING THE Q-DEPENDENCE OF THE NONLINEAR MULTIPLIER

In this appendix, we discuss the microscopic foundations for the phenomenological form of the effective flexoelectric parameters r_i used in Eq. (53). The LC flexoelectric coefficients e_1, e_3 depend on concentration and values of dipoles of the LC molecular components. It is a commonplace observation to note that the electric field acting in the LC cell reorients the LC director. In the context of this paper, it is also helpful to note if the concentration of the LC dipoles is inhomogeneous, then this too is changed by imposing an electric field. Thus, in principle, in an inhomogeneous photorefractive electric field, the flexoelectric coefficients e_1, e_3 will vary with position within in the LC cell.

Now, the equations for the cholesteric director angles (Eqs. (17)–(19)) contain the flexoelectric coefficients. However, these are not now constant but are determined self-consistently together with equations for the LC dipole concentrations. Here, we make an ansatz in which we describe this effect approximately by replacing the true position-dependent flexoelectric coefficients by effective values which depend on the average dipole concentration. The problem remains to understand the dependence of the effective flexoelectric coefficients on the wave number q of the director grating.

Here, we simplify the problem by considering a cholesteric LC with only a single dipole component. Denoting the dipole concentration by $n(\boldsymbol{r})$ and the dipole particle velocity by $\boldsymbol{v}(\boldsymbol{r})$, we can write the dipole flux in an electric field as $n(\boldsymbol{r})\,\boldsymbol{v}(\boldsymbol{r})$ and the dipole flux due to the dipole concentration gradient as $-D\nabla n(\boldsymbol{r})$, where D is a diffusion coefficient. In equilibrium, the total flux is zero, leading to the detailed balance equation

$$n(\boldsymbol{r})\,\boldsymbol{v}(\boldsymbol{r}) - D\nabla n(\boldsymbol{r}) = 0. \tag{C1}$$

Using Stokes' law and the fluctuation-dissipation theorem,[27] we can write

$$\boldsymbol{v} = \frac{D}{k_B T}\boldsymbol{F}, \tag{C2}$$

where $\boldsymbol{F} = (\mathbf{d}\cdot\nabla)\lambda\boldsymbol{E}$ is the force acting on a dipole $\mathbf{d}$ in the external electric field $\boldsymbol{E}$, and where λ is a depolarization parameter which corrects for the difference between the local and imposed electric fields.

Substituting expression (C2) into Eq. (C1), we write the polarization vector as $\mathbf{P}(\boldsymbol{r}) = \mathrm{n}(\boldsymbol{r})\mathbf{d}(\boldsymbol{r})$. Then, projecting Eq. (C1) on the z-axis (the direction perpendicular to the cell substrates) we get

$$\frac{\partial}{\partial z}n = \frac{1}{k_B T}\lambda(\mathbf{P}\cdot\nabla)E_z. \tag{C3}$$

In Ref. 15, we have shown that the contribution to the photorefractive field interaction of the flexoelectric polarization is one order of magnitude larger than that due to the field-induced polarization, $\mathbf{P} = \varepsilon_0\alpha\boldsymbol{E}$. Thus, we can identify $\mathbf{P}(\boldsymbol{r})$ in Eq. (C3) with the flexopolarization vector $\mathbf{P}_f = e_1\mathbf{n}\nabla\cdot\mathbf{n} + e_3(\nabla\times\mathbf{n}\times\mathbf{n})$.[22]

Evidently, an electric field gradient along the x-axis mainly influences the dipole distribution parallel to the cell substrate. To estimate the z-dependence of dipole concentration, we neglect the influence of the electric field gradient along the x-axis (and also of the diffusion along this direction) on the z-dependence of dipole concentration and use instead of Eq. (C3) the simpler equation

$$\frac{\partial}{\partial z}n = \frac{1}{k_B T}\lambda P_{fz}\frac{\partial}{\partial z}E_z. \tag{C4}$$

Using the definition of the cholesteric director angles Eqs. (21)–(26), we can calculate P_{fz}. Then, we substitute P_{fz} and expression for the electric field from Eqs. (13) and (14) into Eq. (C4). After that averaging Eq. (C4) over the x-coordinate, we derive the following equation:

$$\frac{\partial}{\partial z}n = -\frac{ie_3\lambda m}{2k_B T}(iE_{sc})\tilde{q}^2\cos\varphi_0[\theta(z) - c.c.]e^{-\tilde{q}(z+L/2)}. \tag{C5}$$

We solve Eq. (C5) to lowest order by considering the flexoelectric coefficients on the right hand side of Eq. (C5) to correspond to LC in the zero photorefractive field limit. Then, substituting Eqs. (10), (21), and (22) for the director angles into Eq. (C5) and neglecting small terms of order e^{-qL} and e^{-gL} we obtain a solution for the dipole concentration in the form:

$$n(z) = n(0) - \frac{e_3\lambda m^2}{4k_B T}(iE_{sc})^2\tilde{q}^2\mathrm{Im}\frac{[r_1(\tilde{q}^2 - q^2 - 2g^2) - 2r\tilde{q}^2]g + i\tilde{q}[r(\tilde{q}^2 - q^2 - 2g^2) + 2r_1 g^2]}{(\tilde{q}^2 - q^2 - 2g^2)^2 + 4\tilde{q}^2 g^2}$$
$$\times\left[\frac{\tilde{q}(ig+\tilde{q})e^{(i2g-2\tilde{q})(z+L/2)} + (g^2+\tilde{q}^2)e^{-2\tilde{q}(z+L/2)}}{\tilde{q}(g^2+\tilde{q}^2)} + \frac{2(ig - \tilde{q} - \sqrt{q^2+g^2})e^{-(ig+\tilde{q}+\sqrt{q^2+g^2})(z+L/2)} + c.c.}{g^2 + (\tilde{q}+\sqrt{q^2+g^2})^2}\right]. \tag{C6}$$

Equation (C6) describes the inhomogeneity of the flexoelectric coefficients induced by dipole separation in an inhomogeneous photorefractive field.

We now use the effective flexoelectric coefficients, which are proportional to dipole concentration averaging over the total region over which the system is inhomogeneous. Then, averaging $n(z)$ in Eq. (C6) over the area near the cell substrate, $[-L/2,\ -L/2+\Delta]$, we obtain

$$\bar{n} = n(0)\left[1 + \frac{e_3 r\lambda m^2}{16n(0)k_B T g^2}\frac{\tilde{\varepsilon}_\perp + \tilde{\varepsilon}_\parallel}{2\tilde{\varepsilon}_\perp} q^2 F(q)|E_{sc}|^2\right], \tag{C7}$$

where

$$F(q) = \frac{2g^2/r}{\left(\tilde{q}^2 - q^2 - 2g^2\right)^2 + 4\tilde{q}^2 g^2}\left[\frac{4\tilde{q}(\tilde{q} + \sqrt{q^2+g^2})[r(\tilde{q}^2 - q^2 - 2g^2) + 2r_1 g^2]}{g^2 + (\tilde{q} + \sqrt{q^2+g^2})^2}\right.$$

$$-\frac{r[(\tilde{q}^2 - q^2 - 2g^2)(g^2 + 2\tilde{q}^2) - 2\tilde{q}^2 g^2]r_1 g^2(5\tilde{q}^2 - q^2)}{g^2 + \tilde{q}^2} \tag{C8}$$

$$\left.+\frac{2}{3}\Delta^2\{g^2[r_1(\tilde{q}^2 - q^2 - 2g^2) - 2r\tilde{q}^2] - \tilde{q}(\tilde{q} - \sqrt{q^2+g^2})[r(\tilde{q}^2 - q^2 - 2g^2) + 2r_1 g^2]\}\right].$$

The dipole concentration is inhomogeneous in the region in which the inhomogeneous photorefractive electric field acts. Then according to Eq. (14) for the photorefractive electric field, we can substitute in (C8) $\Delta \sim 1/q = \Lambda/2\pi$.

Fig. 5 shows the dependence of the function $F(q)$ on the grating spacing Λ for parameter values used in experiments[16] for the cholesteric mixture BL038/CB15 and for some values of parameter Δ. In the experimental range of Λ, $(0.5, 5)$ μm, $F(q)$ can change appreciably depending on the parameters of system. However, the behavior of $F(q)$ can be approximated by a simpler function $F_1(q) = (1 + \mu_1/q^2)^2$, where μ_1 is used as a fitting parameter.

In result, we can approximate Eq. (C7) for the average dipole concentration near the cell substrate by the formula

$$\bar{n} = n(0)\left[1 + \mu\left(q + \frac{\mu_1}{q}\right)^2 |E_{sc}|^2\right]. \tag{C9}$$

Then, assuming the flexoelectric coefficients to be proportional to the concentration of molecular dipoles, the expression in square brackets of Eq. (C9) describes the q-dependence of effective flexoelectric parameters (see Eq. (53)).

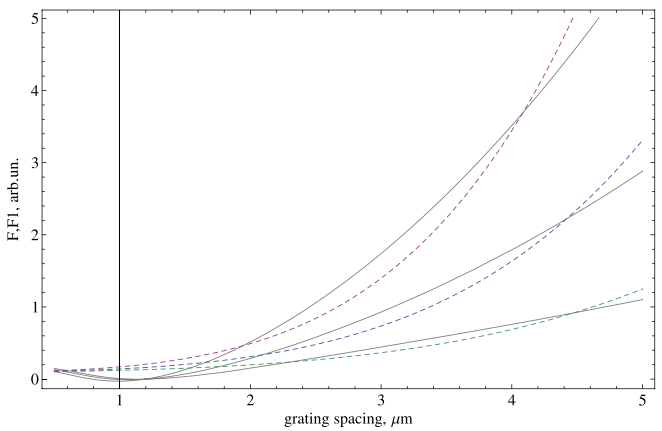

FIG. 5. Dependence of the functions $F(q)$,$F_1(q)$ on grating spacing. Solid curves—$F(q)$ for $\Delta = 0.1/q,\ 0.2/q,\ 0.3/q$; dashed curves $F_1(q) = (1 + \mu_1/q^2)^2$ for $\mu_1 = (0.4,\ 0.75,\ 1.2) \times 10^{13}\text{m}^{-2}$.

[1]E. V. Rudenko and A. V. Sukhov, JETP Lett. **59**, 142 (1994).
[2]E. V. Rudenko and A. V. Sukhov, JETP **78**, 875 (1994).
[3]I. C. Khoo, H. Li, and Y. Liang, Opt. Lett. **19**, 1723 (1994).
[4]A. Brignon, I. Bongrand, B. Loiseaux, and J. P. Huignard, Opt. Lett. **22**, 1855 (1997).
[5]F. Kajzar, S. Bartkiewicz, and A. Miniewicz, Appl. Phys. Lett. **74**, 2924 (1999).
[6]S. Bartkiewicz, K. Matczyszyn, A. Miniewicz, and F. Kajzar, Opt. Commun. **187**, 257 (2001).
[7]G. P. Wiederrecht, B. A. Yoon, and M. R. Wasielewski, Science **270**, 1794 (1995).
[8]I. C. Khoo, B. D. Guenther, M. V. Wood, P. Chen, and M.-Y. Shih, Opt. Lett. **22**, 1229 (1997).
[9]H. Ono and N. Kawatsuki, J. Appl. Phys. **85**, 2482 (1999).
[10]G. Cook, J. L. Carns, M. A. Saleh, and D. R. Evans, Mol. Cryst. Liq. Cryst. **453**, 141 (2006).
[11]R. L. Sutherland, G. Cook, and D. R. Evans, Opt. Express **14**, 5365 (2006).
[12]D. R. Evans and G. Cook, J. Nonlinear Opt. Phys. Mater. **16**, 271 (2007).
[13]N. V. Tabiryan and C. Umeton, J. Opt. Soc. Am. B **15**, 1912 (1998).
[14]D. C. Jones and G. Cook, Opt. Commun. **232**, 399 (2004).
[15]V. Yu. Reshetnyak, I. P. Pinkevych, G. Cook, D. R. Evans, and T. J. Sluckin, Phys. Rev. E **81**, 031705 (2010).
[16]G. Cook, E. Beckel, V. Yu. Reshetnyak, M. A. Saleh, and D. R. Evans, "Controlling light with light: Photorefractive effects, photosensitivity, fiber gratings, photonic materials and more: OSA technical digest (CD)," in *Photorefractive Effects, Photosensitivity, Fiber Gratings, Photonic Materials and More (PR) Squaw Creek, California, October 2007* (Optical Society of America, Washington, DC, 2007).
[17]V. Yu. Reshetnyak, I. P. Pinkevych, G. Cook, D. R. Evans, and T. J. Sluckin, Mol. Cryst. Liq. Cryst. **560**, 8 (2012).
[18]A. D. Kiselev and T. J. Sluckin, Phys. Rev. E **71**, 031704 (2005).
[19]V. A. Belyakov, I. W. Stewart, and M. A. Osipov, Phys. Rev. E **71**, 051708 (2005).
[20]I. Lelidis, G. Barbero, and A. L. Alexe-Ionescu, Phys. Rev. E **87**, 022503 (2013).
[21]P. Yeh, *Introduction to Photorefractive Nonlinear Optics* (Wiley, New York, 1993).
[22]P. G. de Gennes and J. Prost, *The Physics of Liquid Crystals* (Clarendon Press, Oxford, 1993), Chap. 6.
[23]*Handbook of Mathematical Functions With Formulas, Graphs, and Mathematical Tables*, Applied Mathematics Series 55, edited by M. Abramowitz and I. A. Stegun (National Bureau of Standards, , 1972).
[24]F. A. Sala and M. A. Karpierz, Opt. Express **20**, 13923 (2012).
[25]V. A. Belyakov and V. E. Dmitrienko, Sov. Sci. Rev. A **13**, 1–212 (1989).
[26]H. Kogelnik, Bell Syst. Tech. J. **48**, 2909 (1969).
[27]W. Coffey, Yu. P. Kalmykov, and J. T. Waldron, *The Langevin Equation: With Applications to Stochastic Problems in Physics* (World Scientific, 2004), Chap. 1.
[28]N. A. Bailey, D. R. Cairns, G. P. Crawford, and J. N. Hay, Liq. Cryst. **28**, 1761 (2001).
[29]L. M. Blinov, M. I. Barnik, H. Ohoka, M. Ozaki, N. M. Shtykov, and K. Yoshino, Eur. Phys. J. E **4**, 183 (2001).

[30]E. G. Edwards, C. V. Brown, E. E. Kriezis, and S. J. Elston, Mol. Cryst. Liq. Cryst. **400**, 13 (2003).
[31]S. M. Morris, M. J. Clarke, A. E. Blatch, and H. J. Coles, Phys. Rev. E **75**, 041701 (2007).
[32]K. V. Lea, F. Araokaa, K. Fodor-Csorbab, K. Ishikawa, and H. Takezoe, Liq. Cryst. **36**, 1119 (2009).
[33]I. C. Khoo and S. T. Wu, *Optics and Nonlinear Optics of Liquid Crystals* (World Scientific, Singapore, 1993).
[34]T. J. White, S. A. Cazzell, A. S. Freer, D.-K. Yang, L. Sukhomlinova, L. Su, T. Kosa, B. Taheri, and T. J. Bunning, Adv. Mater. **23**, 1389 (2013).
[35]J. Hoogboom, P. M. L. Garcia, M. B. J. Otten, J. A. A. W. Elemans, J. Sly, S. V. Lazarenko, T. Rasing, A. E. Rowan, and R. J. M. Nolte, J. Am. Chem. Soc. **127**, 11047 (2005); Y.-H. Lin, H. Ren, Y.-H. Wu, S.-T. Wu, Y. Zhao, J. Fang, and H.-C. Lin, Opt. Express **16**, 17591 (2008).
[36]L. Zhang, K. Li, W. Hu, Hui Cao, Z. Cheng, W. He, J. Xiao, and H. Yang, Liq. Cryst. **38**, 673 (2011).